SAND2014-4419C

Two dimensional laser-collision induced fluorescence

Low Temperature Atmospheric Pressure Plasmas:

Physics, Diagnostics and Applications

Washington DC, May 29'th 2014

Edward V. Barnat

Sandia National Laboratories

Albuquerque, N.M., United States of America

This work was supported by the Department of Energy Office of Fusion Energy Science
Contract DE-SC0001939

Sandia National Laboratories is a multi-program laboratory managed and operated by Sandia Corporation, a wholly owned subsidiary of Lockheed Martin Corporation, for the U.S. Department of Energy's National Nuclear Security Administration under contract DE-AC04-94AL85000.

LOCKHEED MARTIN

Sandia National Laboratories

Laser-collision induced fluorescence provides measure of electron density and "temperature"

- **Motivation: What is the density? What is the temperature? Where and When?**
  - More traditional probe techniques may couple and perturb
  - Optically passive techniques are line-of-sight limited
  - Optically active-techniques such as Thomson scattering pose their own set of challenges

- **In this presentation**
  - Part I: Laser-collision induced fluorescence (LCIF) primer
    - Collisional-radiative model used to predict LCIF
    - Physics that governs LCIF
  - Part II: Implement and benchmark technique
    - Experimental setup
    - Time evolution of LCIF and time integrated LCIF
  - Part III: Applications of LCIF:
    - Dynamic and structured plasmas
  - Part IV: Future directions and concluding comments
    - Investigate argon

Sandia National Laboratories

LCIF has been considered throughout the years

- **This is LCIF**
  - Laser populates intermediate state
  - Electrons redistribute laser-excited population
  - Monitor changes in emission from coupled states

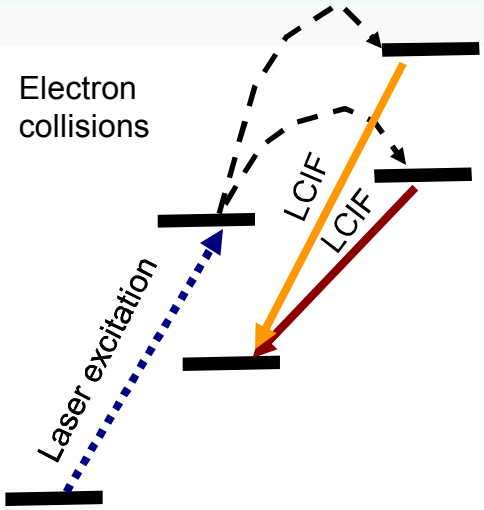

- **Laser-collision based techniques have been considered by many groups**
  - Burrell and Kunze - Collision rates (1978)
  - Tsuchida - First to use for density? (1983)
  - Den Hartog - 1D Sheath (1989)
  - Dzierzega - quasi 2D profiles GEC @ NIST (1996)
  - Stewart - CW LCIF (2002)
  - Nersisyan - He Metastable atmospheric plasma (2004)
  - Krychowiak - TEXTOR (2008)

Work performed at SNL focused on 2D maps of electron densities and temperatures

Ion sheaths

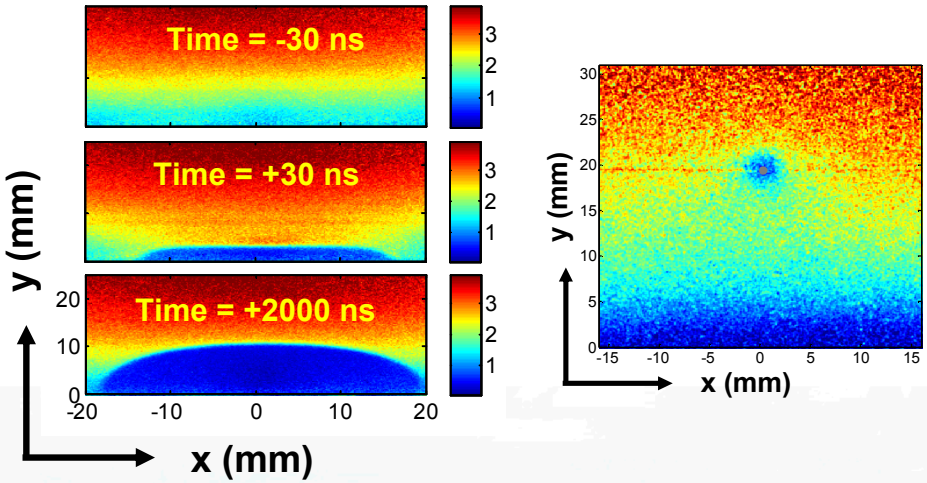

Magnetized plasmas

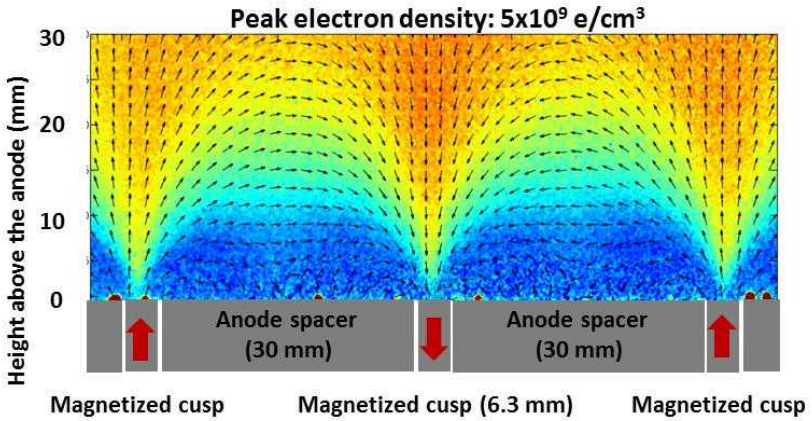

Double layers

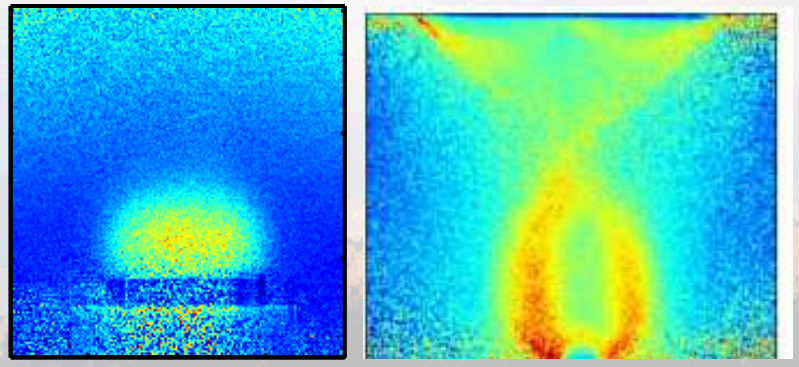

Positive columns

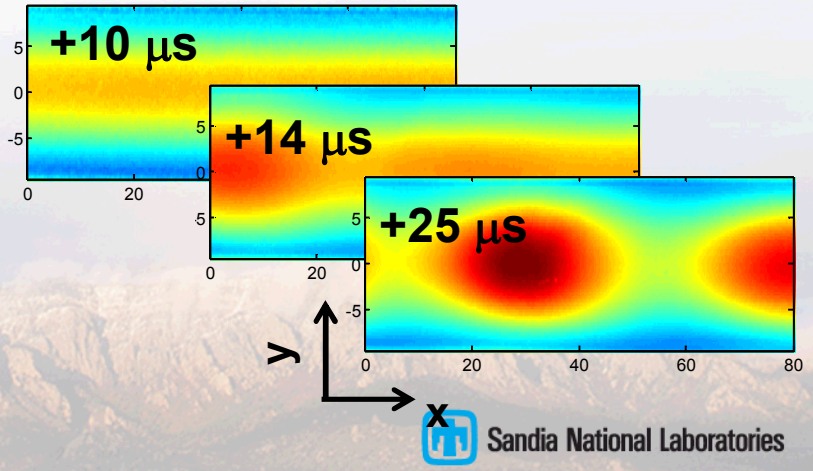

Sandia National Laboratories

Laser-collision induced fluorescence provides measure of electron density and "temperature"

- **Motivation: What is the density? What is the temperature? Where and When?**
  - More traditional probe techniques may couple and perturb
  - Optically passive techniques are line-of-sight limited
  - Optically active-techniques such as Thomson scattering pose their own set of challenges

- **In this presentation**
  - **Part I: Laser-collision induced fluorescence (LCIF) primer**
    - **Collisional-radiative model used to predict LCIF**
    - **Physics that governs LCIF**
  - Part II: Implement and benchmark technique
    - Experimental setup
    - Time evolution of LCIF and time integrated LCIF
  - Part III: Applications of LCIF:
    - Dynamic and structured plasmas
  - Part IV: Future directions and concluding comments
    - Investigate argon

Sandia National Laboratories

Part I: LCIF concepts and physics

- **Overview**
  - LCIF concepts
    - Describe what we look for
  - Key physics
    - Collisional-radiative model to predict LCIF
    - Photon physics that governs excitation and emission
    - Electron physics governs (uphill) inter-state transitions
    - Neutral physics governs (downhill) inter-state transitions

LCIF Concept

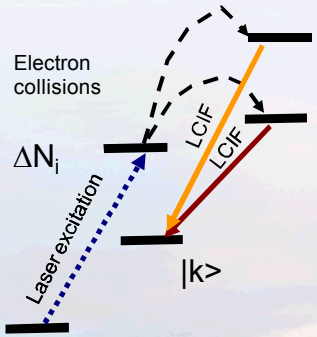

Physics that governs LCIF

CR Model

$$\frac{dN_j}{dt} = \left[\sum_{i \neq j} K_{ij}^e N_i - \sum_{i \neq j} K_{ji}^e N_j\right] n_e + \ldots\ldots$$

Photon physics

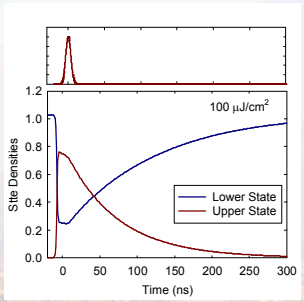

Electron physics

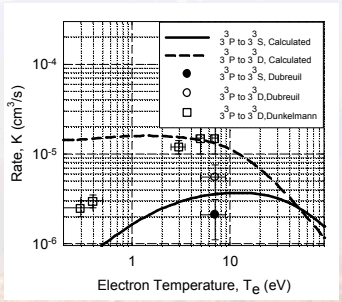

Neutral physics

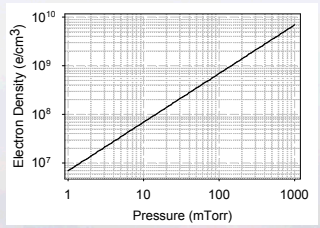

LCIF is based on redistribution of excited state by plasma species (electrons)

- **Pulsed laser excitation causes populates an intermediate state**
  - Relaxation processes deplete excited state
- **Portion of excited state population gets redistributed into "uphill" states**
  - Driven by interaction with energetic plasma electrons

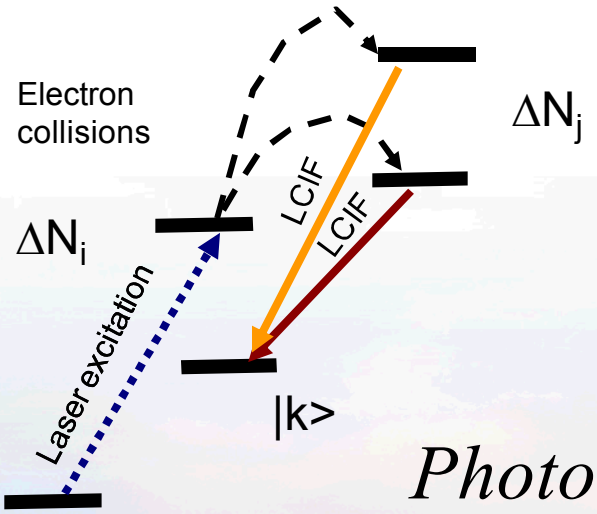

Electron- coupled interaction

$$\Delta N_j \sim K_{ij}^{e} n_e \times \Delta N_i \times \Delta t$$

Change in upper state due to excited state

$$Photons\ emitted \sim A_{jk} \times \Delta N_j \times \Delta t$$

Detected light

LCIF looks for changes in emission of neighboring states after laser excitation

Sandia National Laboratories

Modeling can be used to better estimate excited state redistribution

- **A "good" model is required to predict transfer between levels.**
  - Employ a collisional-radiative model (CRM) to predict redistribution of
- **Sets of coupled equations scale with the number of states needed to be accounted for.**
  - Uncertainties will scale with the number of unknowns
  - Limit sets of interactions that are “most likely” going to impact system response

"Photon mixing" ***"Electron mixing"*** ***"Neutral mixing"***

$$\frac{dN_j}{dt} = \left[\sum_{i>j} A_{ij} N_i - \sum_{i<j} A^j_{ji} N_j\right] + \left[\sum_{i\neq j} K^e_{ij} N_i - \sum_{i\neq j} K^e_{ji} N_j\right] n_e + \sum_k \left[\sum_{i\neq j} K^a_{ikj} N_i - \sum_{i\neq j} K^a_{jki} N_j\right] N_k$$

Absorption and emission

Excitation into and out of states

Redistribution

Complexity of many atomic systems
LCIF "challenging"

- **Atomic structure will govern which pathways are accessible for LCIF**
  - **Which states radiate, and are they uniquely detectable**

Hydrogen

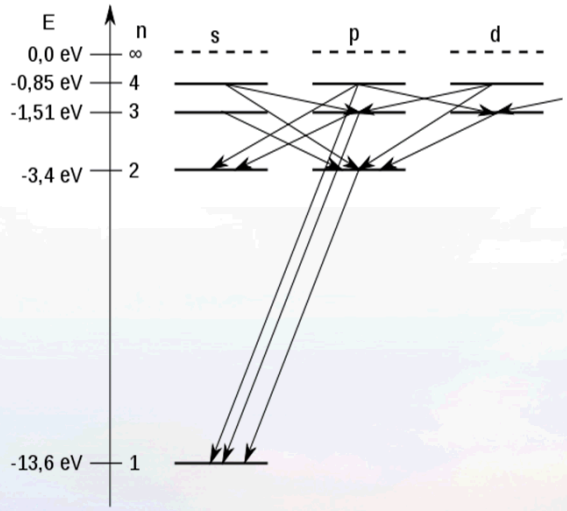

http://commons.wikimedia.org/wiki/File:Grotrian_H.svg

Helium

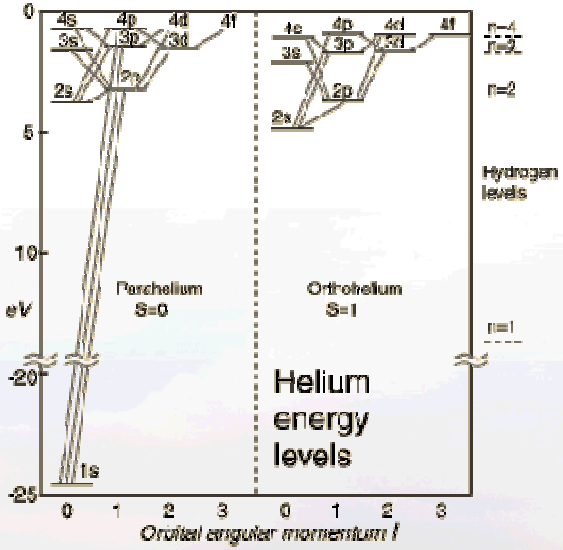

http://hyperphysics.phy-astr.gsu.edu/hbase/quantum/helium.html

Argon

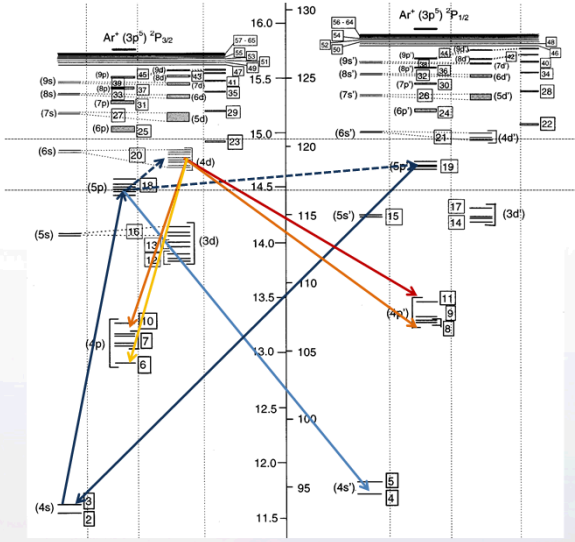

Taken from Bogearts et. al, J. Appl. Phys. **84**, 121, 1998

The number of interactions that need to be accounted for scales with complexity of the system

Helium atom serves as target species for LCIF measurements

- **Limited excitation/ de-excitation pathways.**
  - Hydrogen is simpler, but restricted pathways.
  - Neon, Argon, etc… more complex structure.
- **Cross-sections between states are well known.**
  - Inter-state transitions between high lying states are known for helium.
- **Most of my studies have been performed from the triplet manifold.**
  - Well isolated from the singlet system – electron interaction rates small.
  - 2^3S metastable states serves as a useful reservoir to excite from.
- **Specifics will change from specific excitation path or atomic system**
  - General concepts are expected to hold

Sandia National Laboratories

Key photon-based physics

- **Discussion of key photon-based physics**
  - Absorption and laser rate equation
  - State population after excitation
  - Spontaneous emission and radiation trapping

"Photon mixing"

$$\frac{dN_j}{dt} = \left[\sum_{i>j} A_{ij} N_i - \sum_{i<j} A_{ji}^{j} N_j \right]$$

Sandia National Laboratories

Laser excitation initiates and dictates systems evolution

- **Laser excitation initiates population transfer**
  - Moves population from base state to state of interest
- **Behavior of the laser dictates what states are accessed and for how long**
  - Considering laser that is Gaussian in spectral and temporal outputs.

Governing rate equation

$$\frac{dN_u}{dt} = A\left(\frac{\lambda^2}{8\pi}\right)\left(N_L - \frac{g_U}{g_L}N_U\right)\left\langle g(\nu)\frac{I(\nu,t)}{h\nu}\right\rangle - \sum AN_U$$

A – Einstein coefficient connecting upper and lower states
λ, ν – Wavelength and frequency of the transition
$N_{L,U}$ – Densities of the coupled states
$g_{L,U}$ – degeneracy of the coupled states
$g(\nu)$ – line shape of the transition
I – Intensity profile of the laser

Temporal profile **Spectral profile**

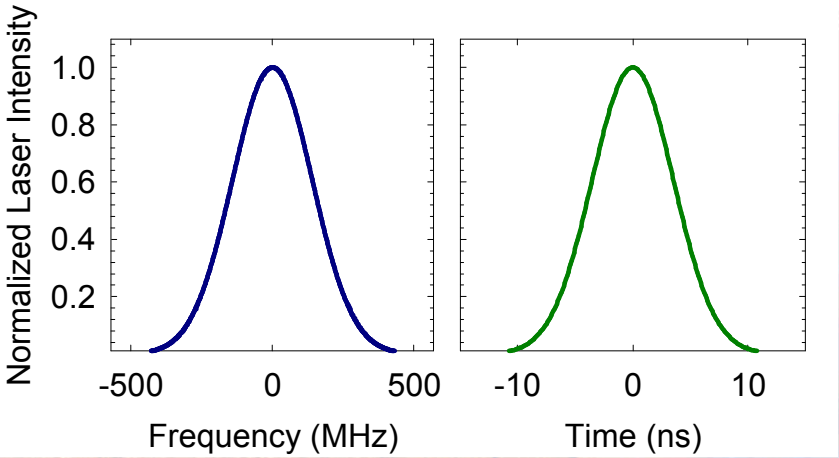

Specifics will change but principles will hold

Sandia National Laboratories

The absorption interaction is described by the line shape of the transition

- Motion of the absorbing species and interactions of these species govern line shape g(ν)
  - Doppler, Vander Waal's, Stark
- Actual line shape is typically a convolution of these different interactions
  - Lorentz × Gaussian ~ Voigt

Functions used to describe line shape

Lorentzian:

$$g(\upsilon) = \frac{\Delta\upsilon_L}{2\pi\left((\upsilon-\upsilon_0)^2 + \left(\frac{\Delta\upsilon_L}{2}\right)^2\right)}$$

Gaussian:

$$g(\upsilon) = \left(\frac{4ln2}{\pi}\right)^{0.5} \frac{1}{\Delta\upsilon_D} e^{\left[-4ln2\left(\frac{\nu-\nu_0}{\Delta\upsilon_D}\right)^2\right]}$$

$$\Delta\upsilon_D = \left(\frac{8\pi kTln2}{Mc^2}\right)^{1/2}$$

Representative line shape

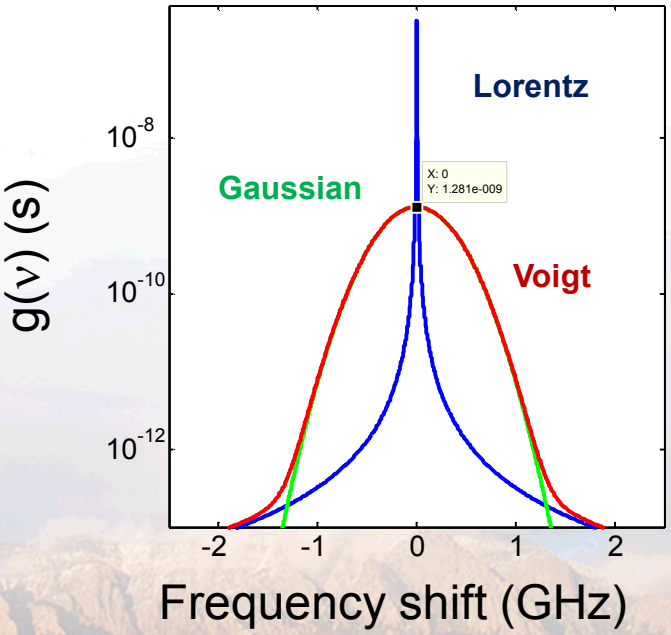

Conditions will govern which interaction may dictate

Sandia National Laboratories

Pressure broadening can dictate absorption profiles

- **At higher pressures, collisional "pressure" broadening can dictate absorption profiles**
  - Broadeing ~ 10 MHz/Torr (12 MHz/Torr Helium, 20 MHz/Torr Argon)
  - Shifting ~ 1 MHz/Torr
- **Width of absorption profiles can exceed laser excitation profiles**
  - Less effective excitation <g(ν)I(ν)>

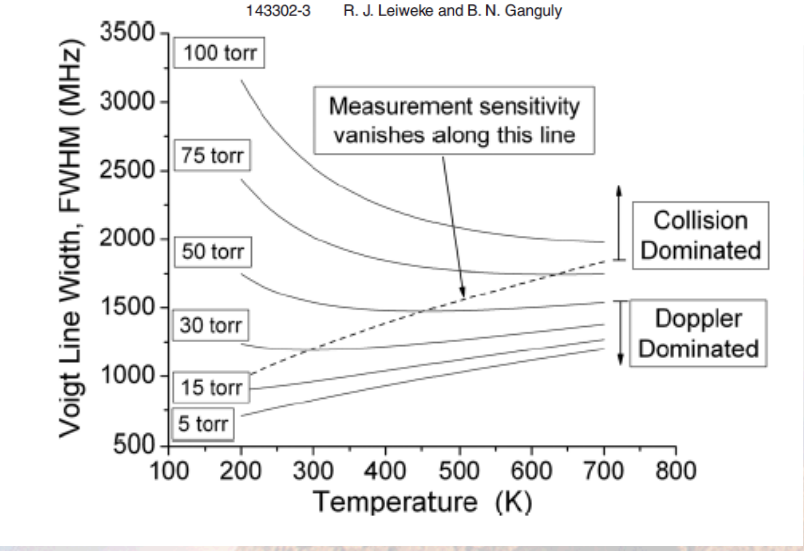

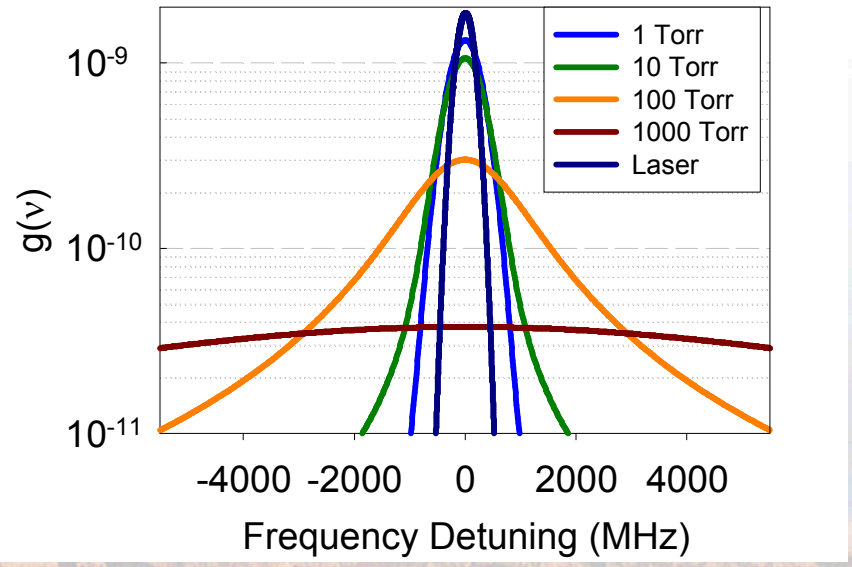

For modest pressures g(ν) ~ 10^{-10} to 10^{-9} s

Examples of laser excitation – Helium

- **Laser excitation initiates population transfer into the 3^3P state**
  - Incorporate temporal profile of the pulse.
- **Photon intensity governs degree of population transfer**
  - Photon intensities ~ 100 μJ/cm²

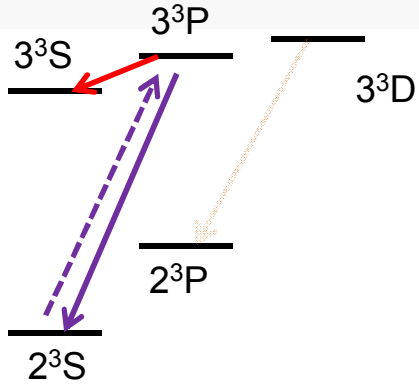

Temporal evolution of states

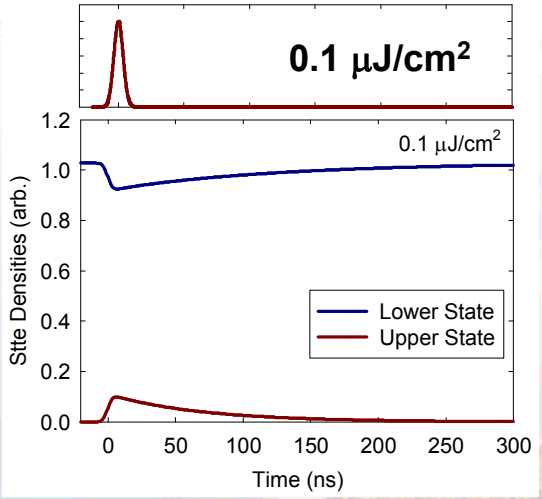

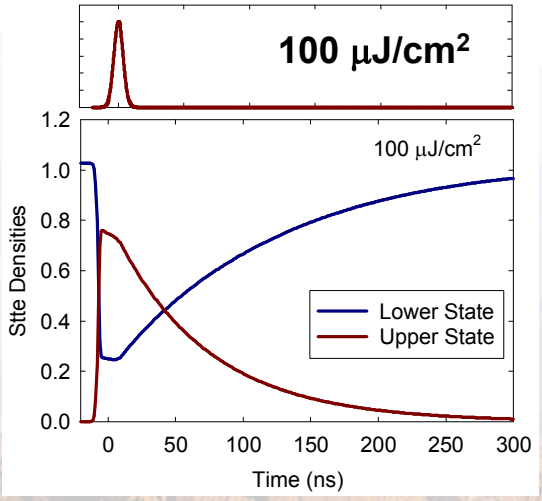

Post-excitation Densities

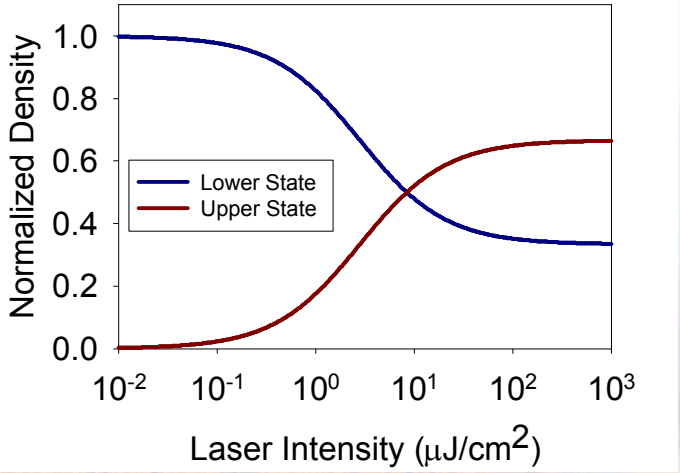

Strong laser excitation depletes lower states for limited time

Sandia National Laboratories

Response after 2^3S -> 3^3P excitation

- **Other states that are radiativly coupled to the excited state will become populated**
  - Degree of population depends on the strength (*A*) of the radiative coupling.

Excitation of $2^3S \rightarrow 3^3P$

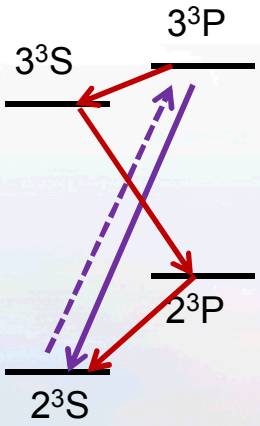

Transition	λ (nm)	A (×10⁷ s⁻¹)
3^3P -> 2^3S	388.9	0.948
3^3P -> 3^3S	4296	0.107
3^3S -> 2^3P	706.5	2.78
2^3P -> 2^3S	1083	1.02

Population of coupled states

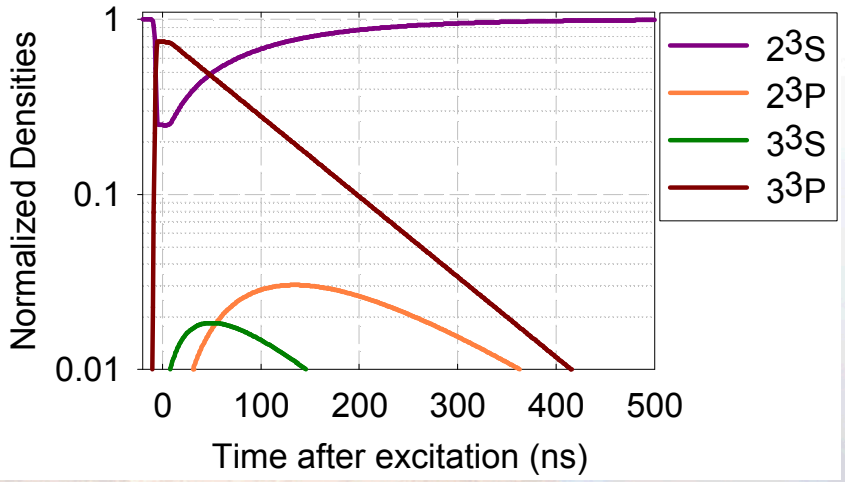

Lower states will become populated, depending on decay channels

Response after 2^3P -> 4^3S excitation

- **In some instances, lower state populations can exceed upper state populations**
  - Longer lived (smaller A) states can act as a reservoir for excited states

Excitation of $2^3P \rightarrow 4^3S$

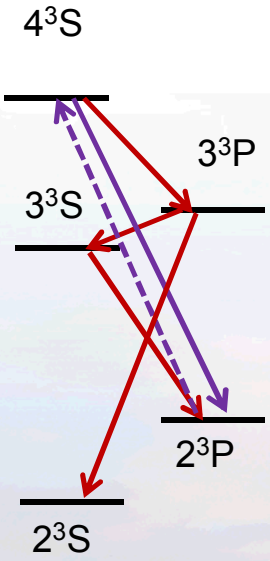

Transition	λ (nm)	A (×10⁷ s⁻¹)
4^3S -> 2^3P	471.3	1.06
4^3S -> 3^3P	2113	0.65
3^3P -> 2^3S	388.9	0.948
3^3P -> 3^3S	4296	0.107
3^3S -> 2^3P	706.5	2.78

Population of coupled states

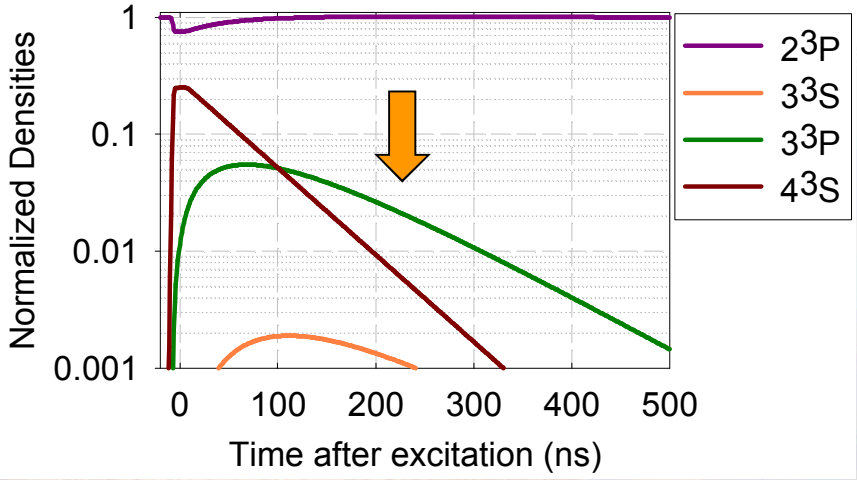

Coupling into lower lying states can impact where collisions can occur

Sandia National Laboratories

Caution on behavior between radiativly coupled states

- **Initial studies utilized the radiation from the 3^3S to quantify population of the 3^3P**
  - It was not thought desirable to interrogate LIF at same wavelength used to excite
- **Time dependent LIF from the 3^3S did not agree with anticipated response**
  - Little to no delay between 3^3P excitation and 3^3S radiation

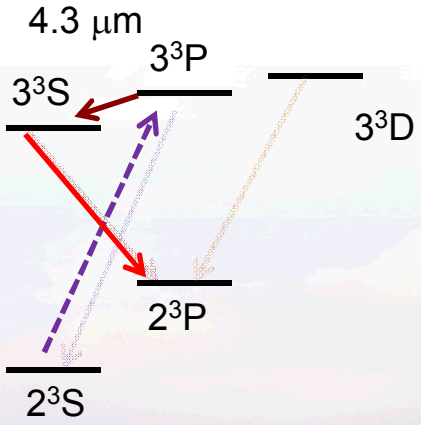

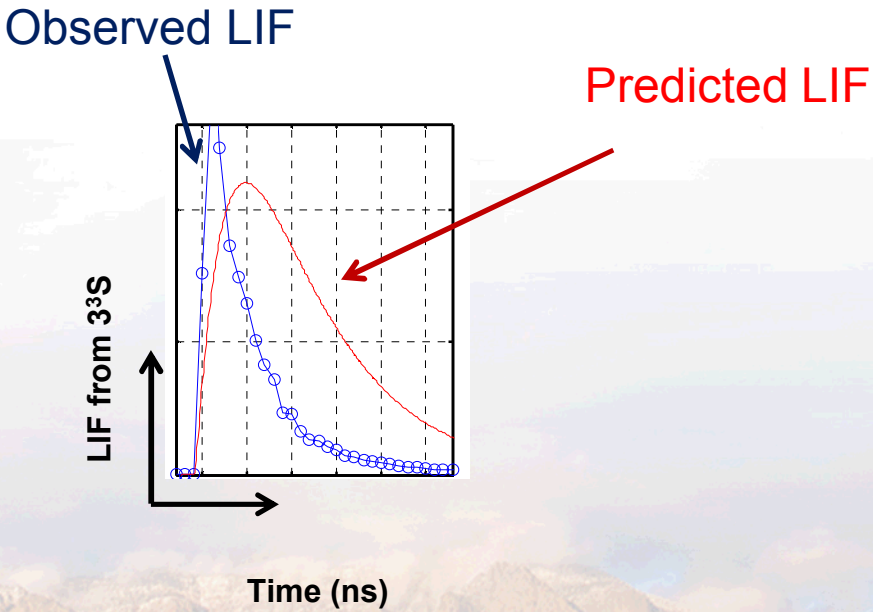

Stimulated emission due to strong population inversion was observed

Base laser-rate equation:

Spontaneous Emission ***Stimulated emission & absorption***

$$\frac{dN_S}{dt} = AN_P + A\left(\frac{\lambda^2}{8\pi}\right)g(\nu)\left(N_P - \frac{g_2}{g_1}N_S\right)\frac{I}{h\upsilon}$$

After pumping inversion occurs:

$$\frac{dN_S}{dt} \approx A_{eff}N_P, \quad N_P >> N_S$$

Where

$$A_{Eff} = A\left[1 + \left(\frac{\lambda^2}{8\pi}\right)g(\nu)\frac{I}{h\upsilon}\right] > 10^8 s^{-1}\,?$$

Photon density ***Gas density***

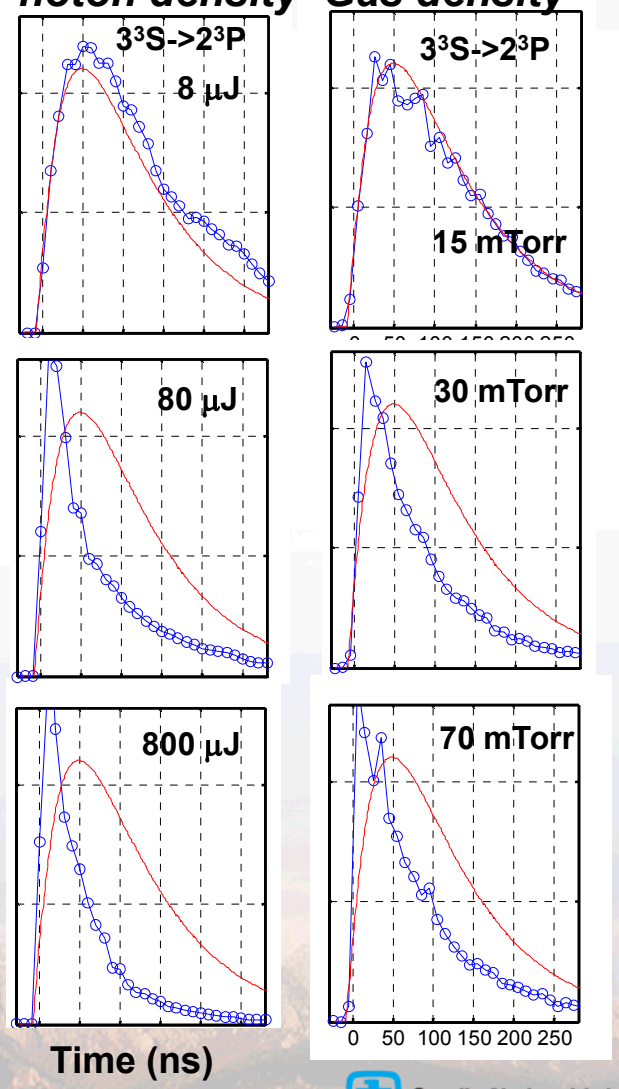

Sandia National Laboratories

Complete treatment bypassed through simplifying approximations

- **Assume population inversion occurs only during laser excitation**
  - Side step need to track absolute photon intensities

$$A_{Eff} = A_{Nom}\left[1 + A_{Inv}e^{-\frac{I_{Laser}}{I_{Threshold}}}\right]$$

Normalized time resolved trends

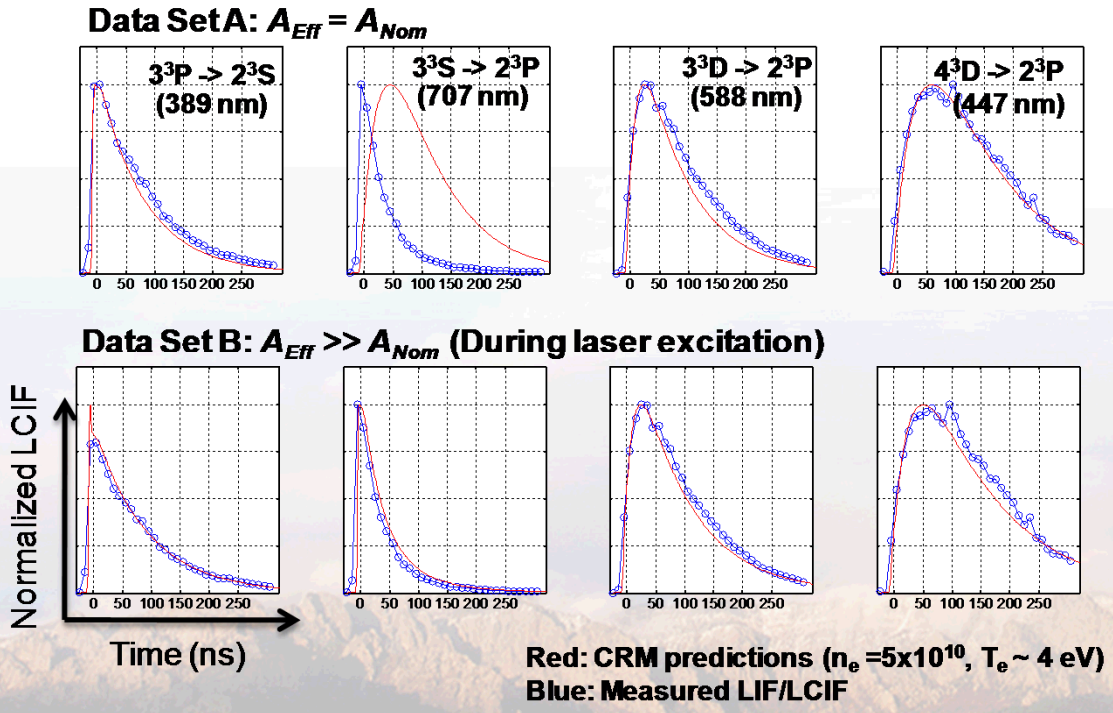

Simplifying assumption produces trends consistent with observation

Sandia National Laboratories

Radiation trapping can impact measurements

- **Excitation from helium metastable is quite advantageous at low pressures**
  - Highly populated, long lived 2^3S metastable state
  - Well known cross-sections

- **As density increases and as composition changes**
  - Radiation trapping/transport becomes problematic

$$\tau = L / l_{mfp} \approx f_{nm} \lambda \left(Mc^2 / kT_A \right)^{1/2} N_A L << 1$$

Transition	f_{nm}	τ
$3^3P \rightarrow 2^3S$	0.064	>1
$4^3P \rightarrow 2^3S$	0.02	~1

(Assuming L=1 cm and $N_A \sim 10^{13}$ absorbers/cm^3)

States connected to 2^3S can become trapped do to strong coupling and higher populations

Consider densities of lower states and mean free-paths of photons traversing the plasma

- **At higher pressures and densities, 2^3P state becomes adequately populated**
  - Comparable oscillator strengths (into comparable levels)
  - Sufficiently lower population compared to 2^3S

Scaling

2^3S State:

$$n_{2(3)S} \sim \frac{K^e_{0->S}}{K^e_{S->P}} n_0 \sim 10^{-5} n_0$$

2^3P State:

$$n_{2(3)P} \sim \frac{1}{A_{P->S}} \left[K^e_{0->P} + K^e_{S->P}\right] n_0 n_e$$

Trends

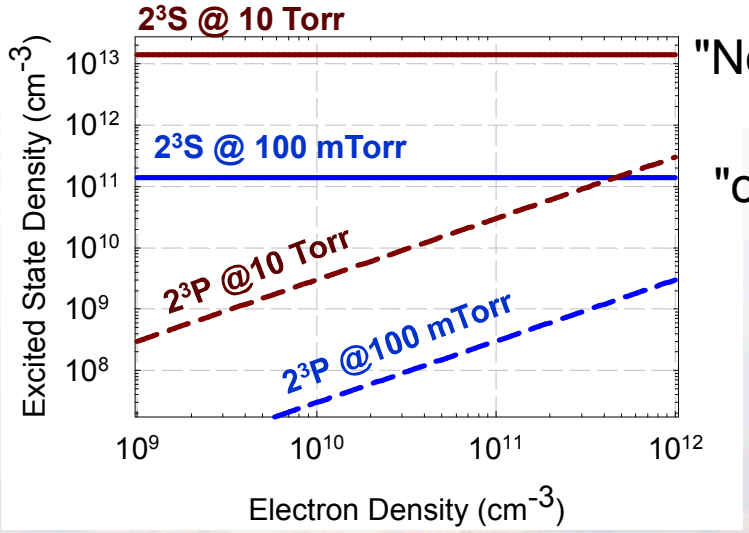

Low 2^3P state densities should be high enough to pump but low enough not to trap

Sandia National Laboratories

Key electron-based physics

- **Discussion of key electron-based physics**
  - Cross-sections, electron energy distribution functions and rates
  - Population dynamics after laser excitation
- **Consider these effects in conjunction with radiative decay**
  - Account for temporal redistribution and decay of electron-driven interactions

"Electron mixing" with radiative decay

$$\frac{dN_j}{dt} = \left[\sum_{i\neq j} K^e_{ij} N_i - \sum_{i\neq j} K^e_{ji} N_j\right] n_e + \left[\sum_{i>j} A_{ij} N_i - \sum_{i<j} A^j_{ji} N_j\right]$$

Sandia National Laboratories

Electron-atom coupling is governed by collisions between an inbound electron and excited atom

- **Cross-sections are used to describe the probability that an excited state will be redistributed else-where**
  - Complex functions of inbound energy and the quantum mechanics of the driven transition.
  - Approximate expressions are useful ($1/\Delta E^2$ Born-based approximations) but limited in the ranges applicable to LCIF (0.1 → 10 eV).

Representative cross-sections

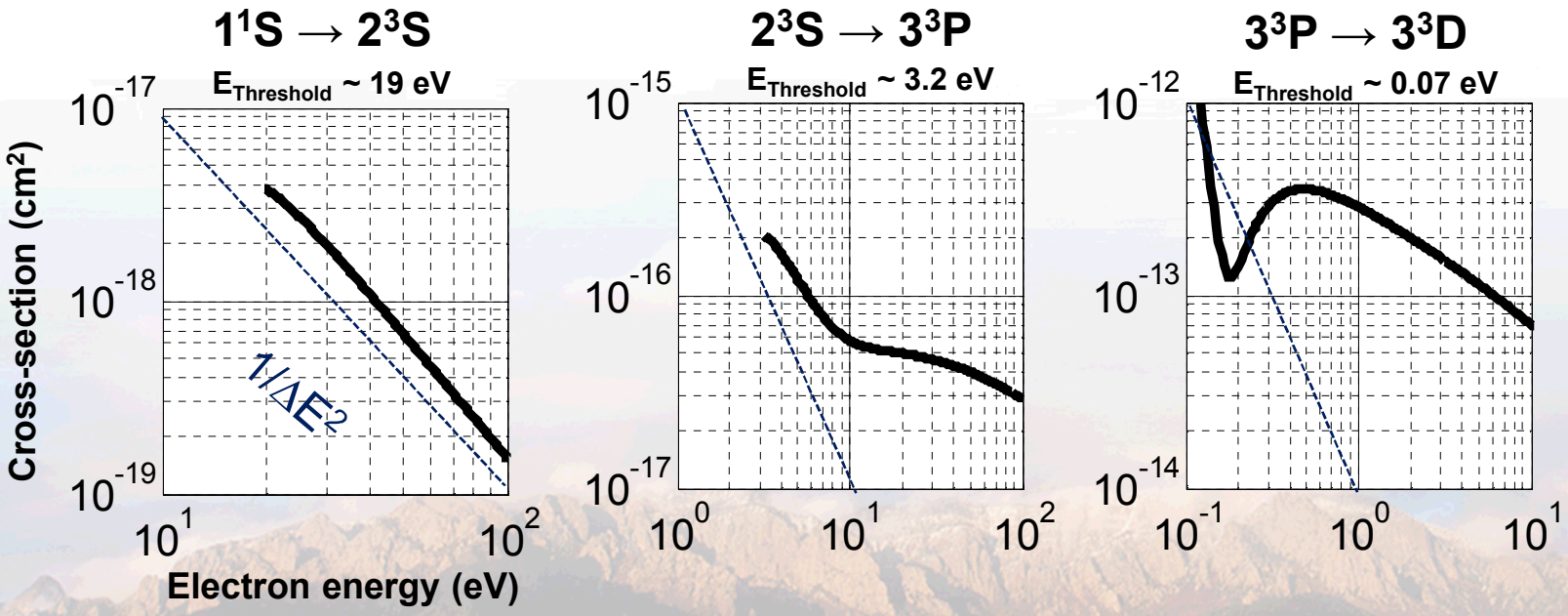

1: Yu. Ralchenko, R. K. Janev, T. Kato, D. V. Fursa, I. Bray, F. J. De Heer, Atomic Data and Nuclear Data Tables **94**, 603 (2008)

Sandia National Laboratories

Super-elastic collisions need to likewise be considered

- **Super-elastic collisions are also permissible and should be accounted for in accurate book-keeping**
  - Electrons drive excited states to lower energy levels (and get heated)
- **Klein-Rosseland approximation**

$$K_{ij}^{e} = \langle \sigma_{ij} v_e \rangle = \left(\frac{m_e}{2\pi k T_e} \right)^{3/2} \int_0^{\infty} \sigma_{ij}(v) \exp\left(\frac{-m_e v^2}{2 k_B T_e} \right) 4\pi v^2 dv \left[\frac{g_j}{g_i} \exp\left(\frac{(E_j - E_i)}{k_B T_e} \right) \right]$$

Comparison of forward and reverse cross-sections

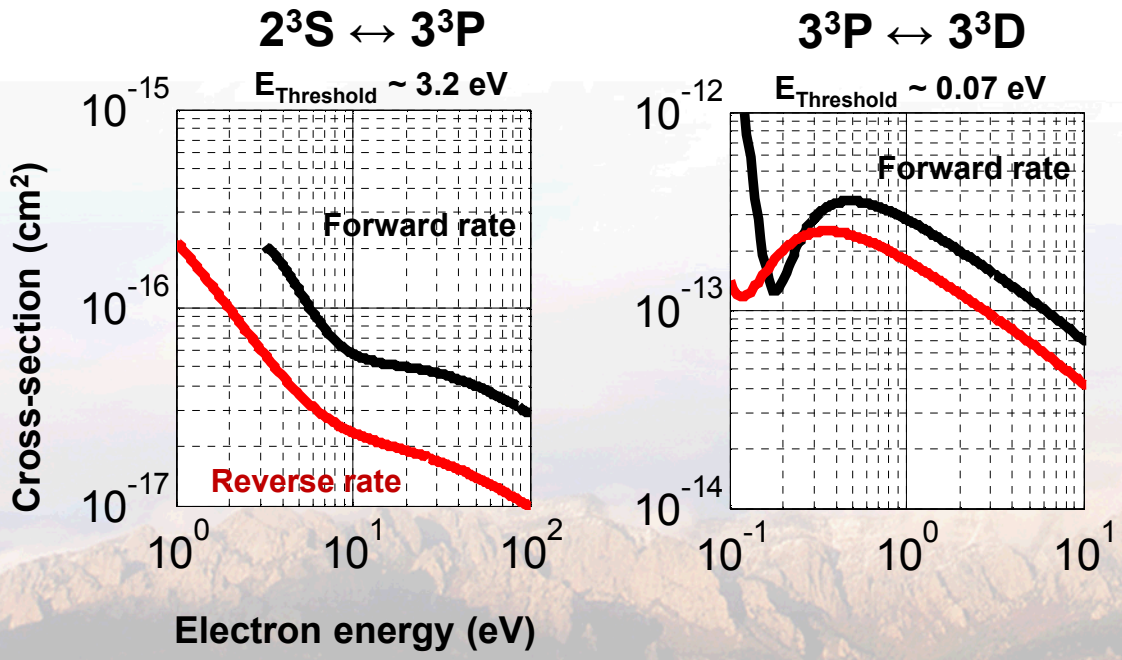

Sandia National Laboratories

Energy spectrum of the electrons is needed to predict LCIF induced by electron collisions

- The collision rate (K^e_{ij}) is utilized in the CRM to account for electron-excited state collisions.

$$\Delta N_j \sim K^e_{ij} n_e \times \Delta N_i \times \Delta t$$

- The rate is computed by taking the weighted average of the cross-section and the velocity.

$$K^e_{ij} = \left\langle \sigma_{ij}(E) v_e(E) f(E) \right\rangle$$

- Where the weighting "function" (*f(E)*) is the electron energy distribution function (EEPF).

Maxwellian distribution

$$EEPF \sim \sqrt{E/kT_e{}^3}\; e^{-E/kT_e}$$

where

$$1 = \int dE \sqrt{E/kT_e{}^3}\; e^{-E/kT_e}$$

Representative distributions

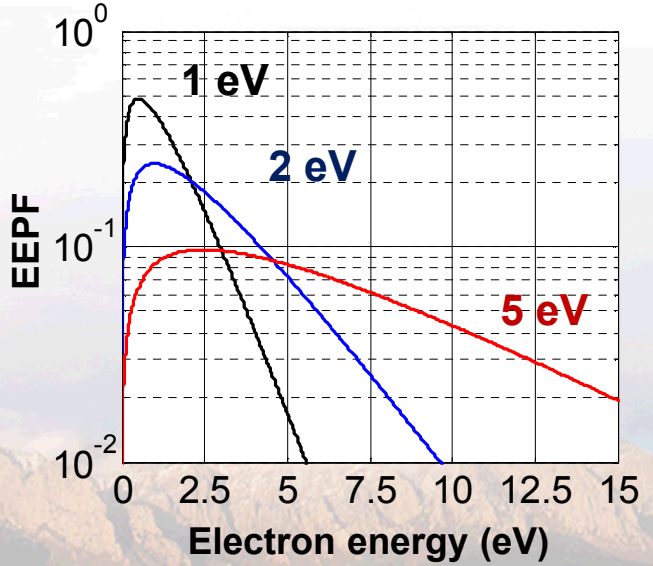

Sandia National Laboratories

Weighted sum of the electron velocity and the cross-section yields the collision rates

- **Functional dependence of collision rates are computed as a function of "effective" electron temperature**
  - Explicit dependence on EEPF is discussed elsewhere

Key transitions

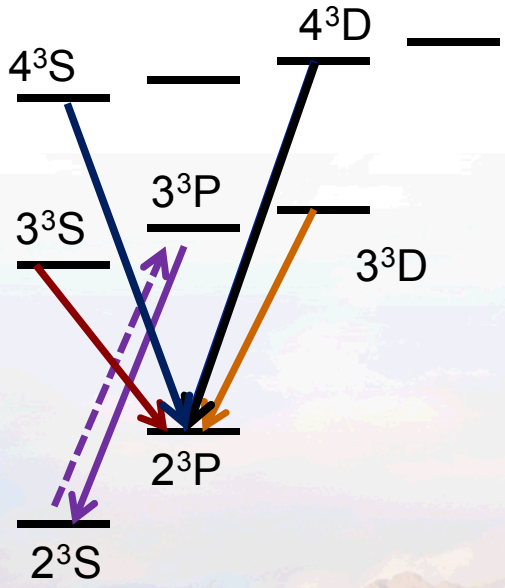

Key Rates

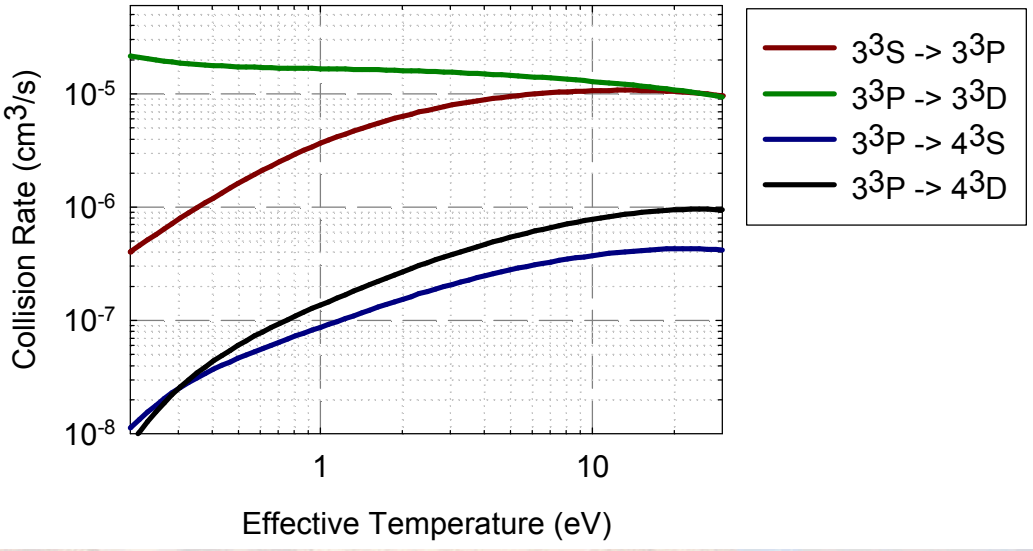

Sandia National Laboratories

Comparison of anticipated rates to observed rates helps benchmark diagnostic

- **Utilize functionalized form of cross-sections compiled by Ralchenko[1]**
  - Integrate to get rates, compare to measured rates [2,3]

Key transitions

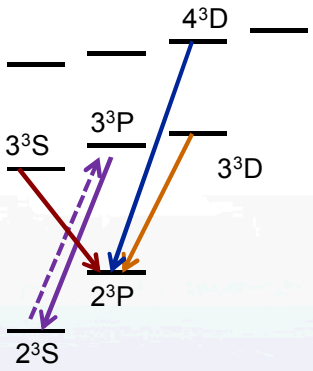

Computed and measured excitation rates in Helium

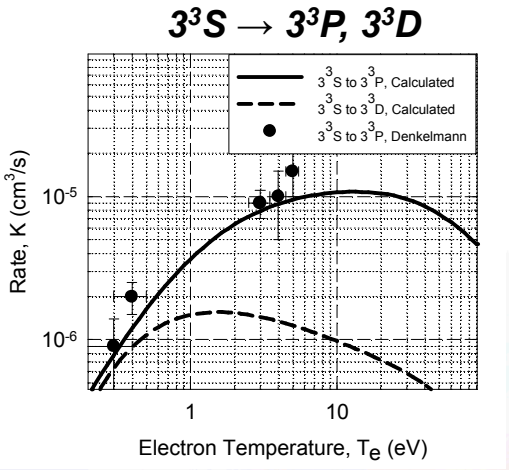

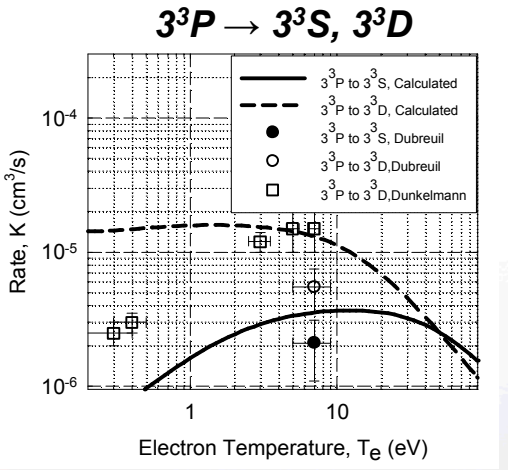

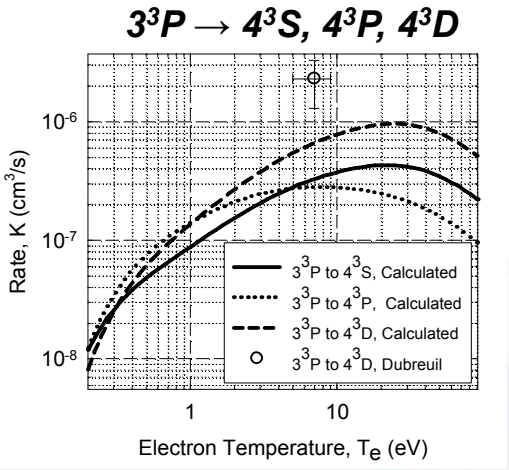

1: Yu. Ralchenko, R. K. Janev, T. Kato, D. V. Fursa, I. Bray, F. J. De Heer, Atomic Data and Nuclear Data Tables **94**, 603 (2008)
2: R. Denkelmann, S.Maurmann, T. Lokajczyk, P. Drepper, and H. –J. Kunze, J. Phys. B: At. Mol. Opt. Phys. **32**, 4635 (1999).
R. Denkelmann, S. Freund and S. Maurmann, Contrib. Plasma Phys. **40**, 91 (2000).
3: B. Dubreuil and P. Prigent, J. Phys. B: At. Mol. Opt. Phys. **18**, 4597 (1985).

Accuracy of n_e, T_e depend on knowledge of $K_{ij}(kT_e)$

Sandia National Laboratories

Small energy gap leads to "kT_e independent" coupling of 3^3P to 3^3D

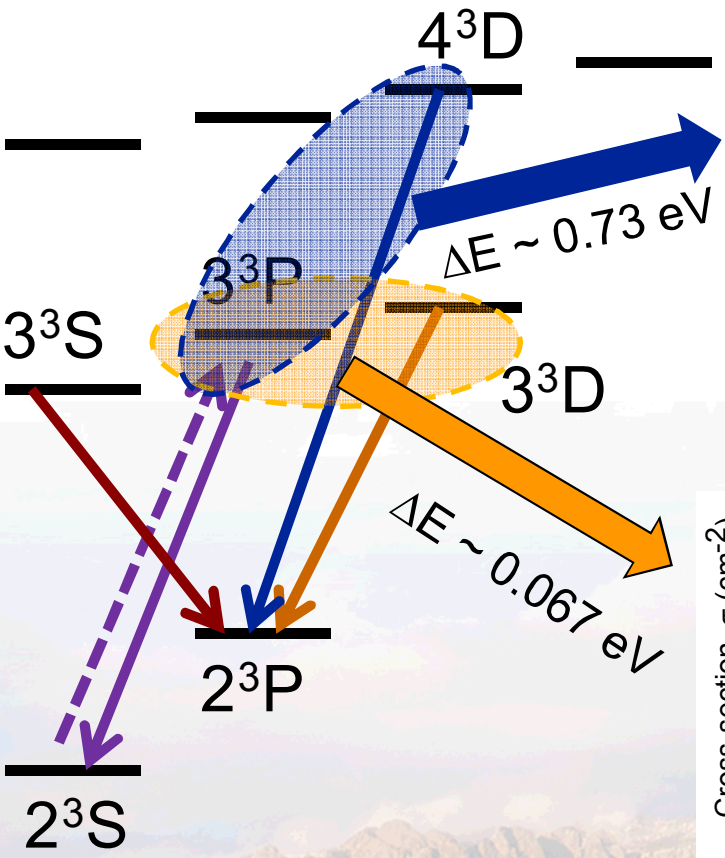

$3^3P \rightarrow 4^3D$

Cross-sections

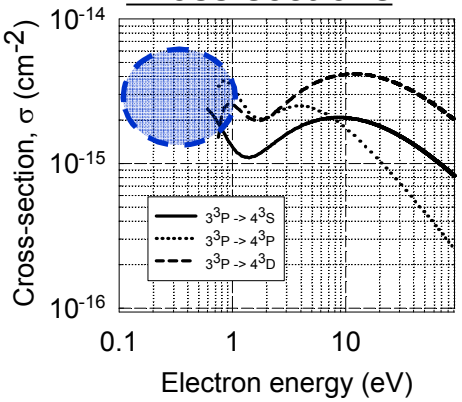

Rates

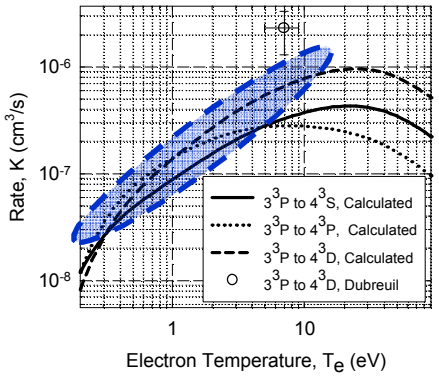

$3^3P \rightarrow 3^3D$

Cross-sections

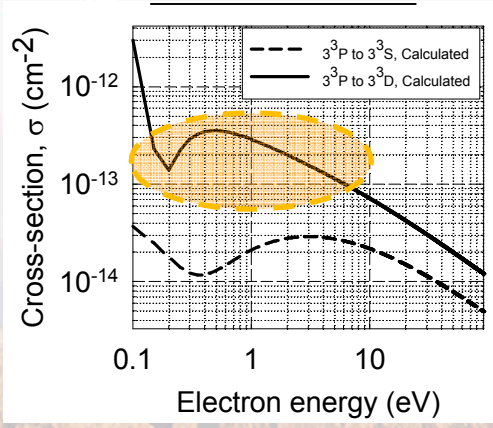

Rates

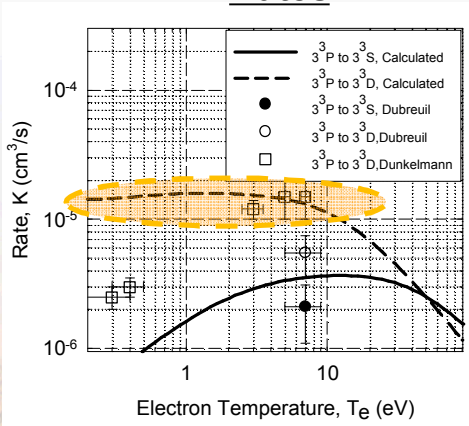

Considerable fraction of the electrons are capable of driving the interaction

Yu. Ralchenko, R. K. Janev, T. Kato, D. V. Fursa, I. Bray, F. J. De Heer, Atomic Data and Nuclear Data Tables **94**, 603 (2008)

Electron-induced collisions are observable in energetically "up hill" transitions

- **Solution of the CRM including both electrons and radiative decay.**
  - Electrons redistribute excited state to near by states
- **There are two key-observables obtained from these simulations**
  - Degree of re-distribution scales with collision rate (n_e, T_e)
  - Lifetime of excited states become truncated at higher densities

Key transitions

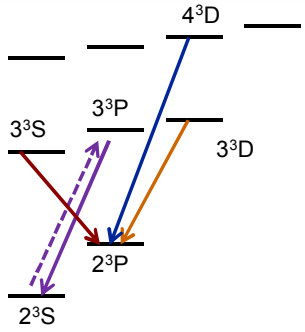

Representative state populations after excitation

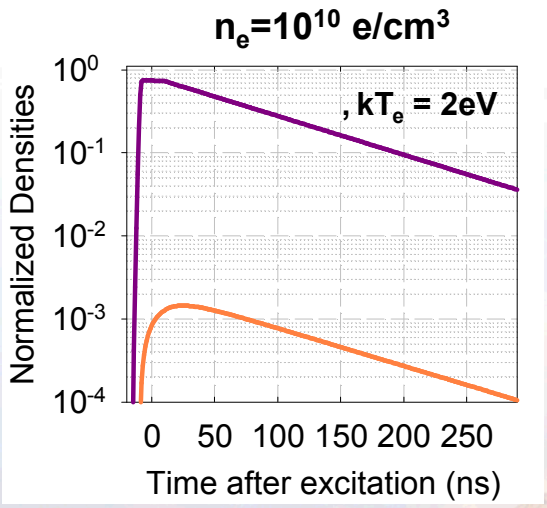

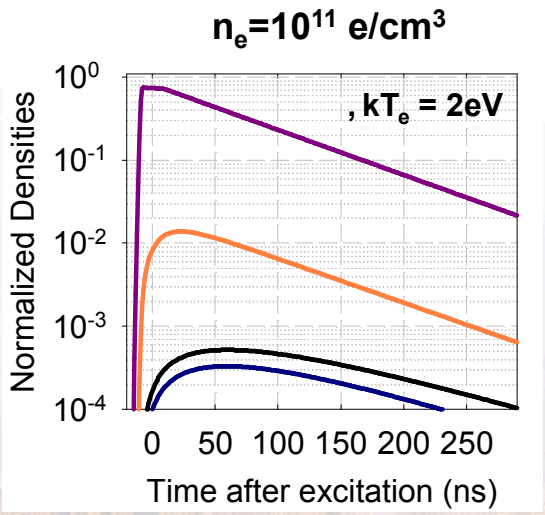

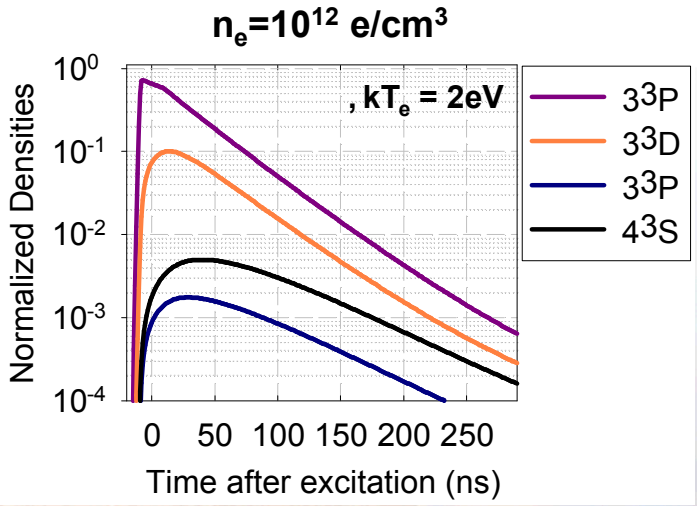

Sandia National Laboratories

Lifetime of the states impacted when excitation rates become comparable to radiadiative rates

- **Lifetime becomes reduced as electron impact begins to compete with radiative relaxation**
  - Life-time reduction serves to quantify collisional rate (Kn_e)

$$K_{ij}^{e} n_e \sim A_{ij} \quad \Rightarrow \quad 10^{-5} \times 10^{11} \sim 10^{7}$$

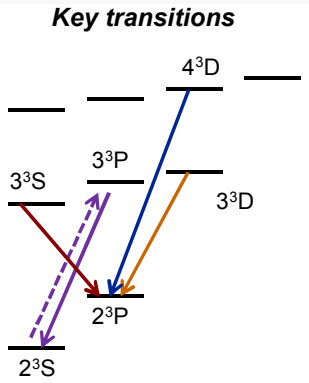

Computed temporal evolution

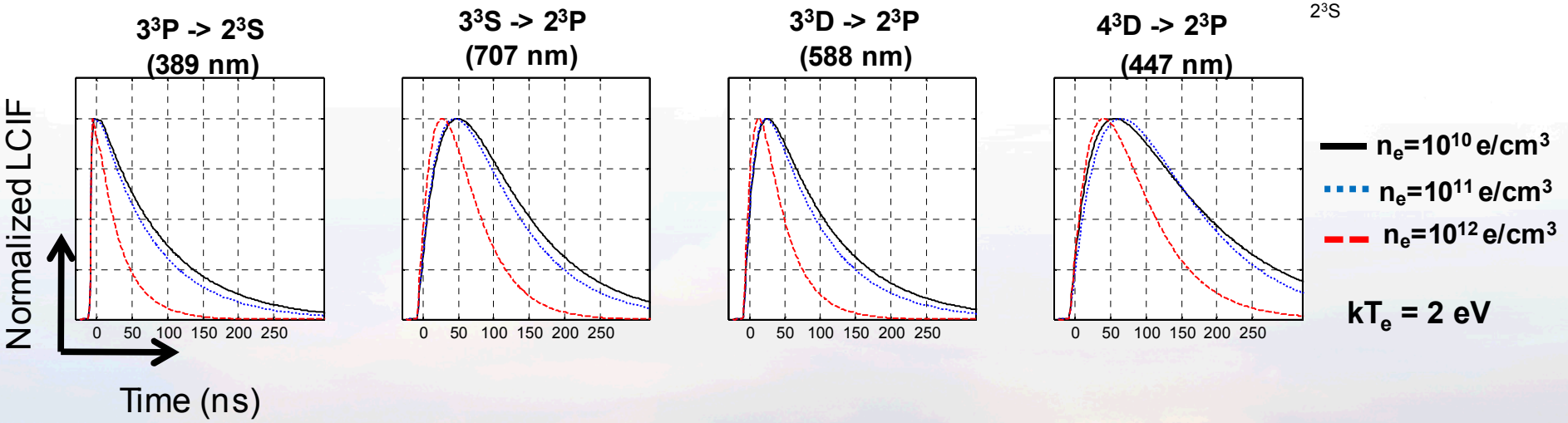

Sandia National Laboratories

Temporal integration of light detected serves to simplify LCIF implementation

- **Examine ratios of time integrated LCIF**
  - Time integration usually chosen to be shortly after excitation
- **Eliminates need for absolute calibrations**
  - Still need relative efficiencies of imaging system

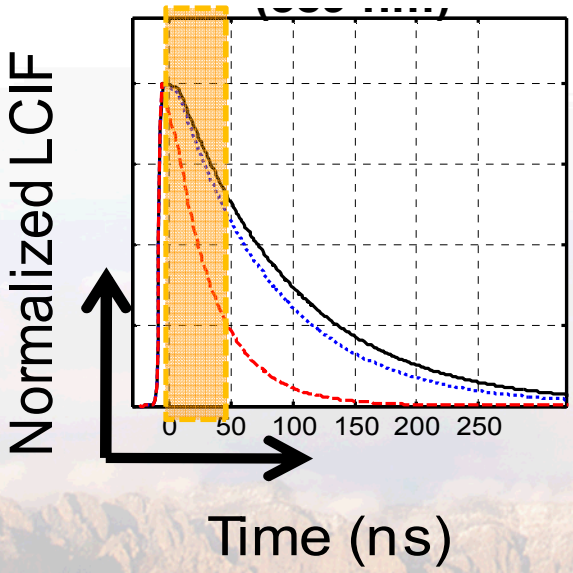

Ratio of LCIF to LIF yields electron induced excitation rates

- **Ratios constructed from LCIF and LIF from the laser excited state yields rates**
  - Eliminated dependence of exact knowledge of how much excited state was generated

Ratio between LCIF and LIF

$$\frac{\Delta N_j}{N_{3^3P}} \sim K^e_{3^3P->j} n_e \times \Delta t$$

Ratio of LCIF to 389 nm LIF

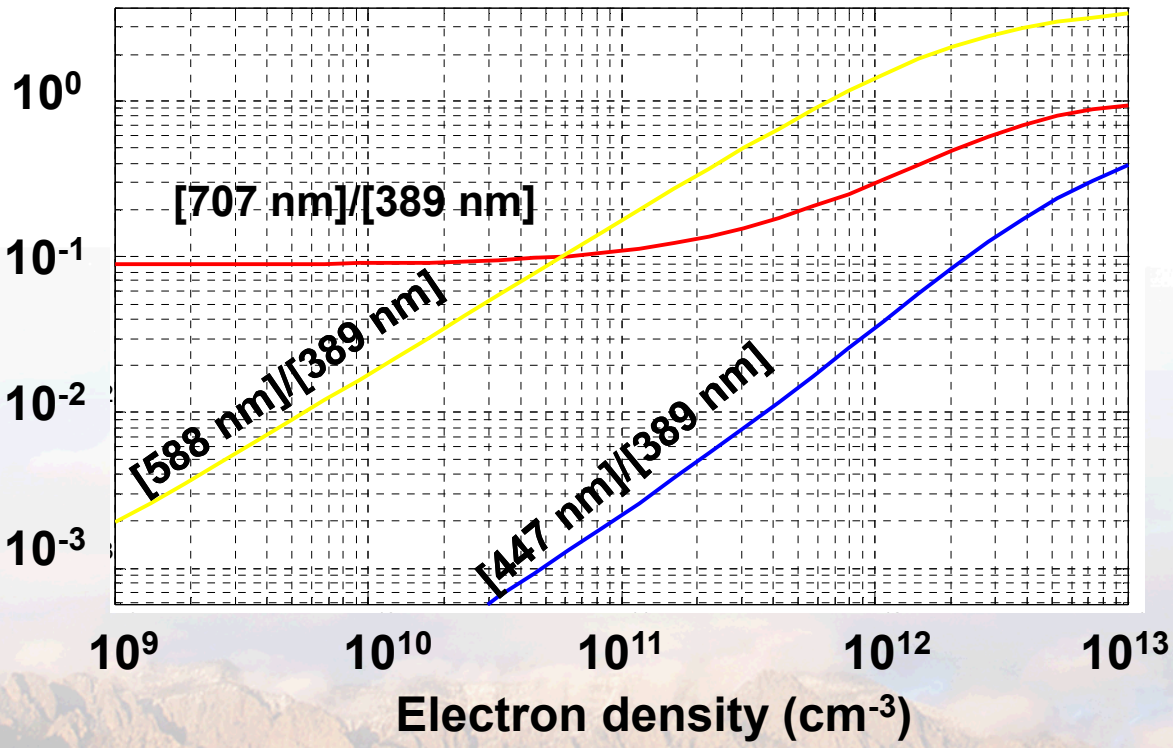

Sandia National Laboratories

Ratios of various LCIF lines can serve as a measure of effective temperature

- **Ratios constructed from two LCIF measurements yields ratio of two rates**
  - Elimination of electron density dependence.

Ratio between two LCIF signals

$$\frac{\Delta N_j}{\Delta N_i} \sim \frac{K^e_{0j}}{K^e_{0i}}$$

Ratio [447 nm]/[588 nm]

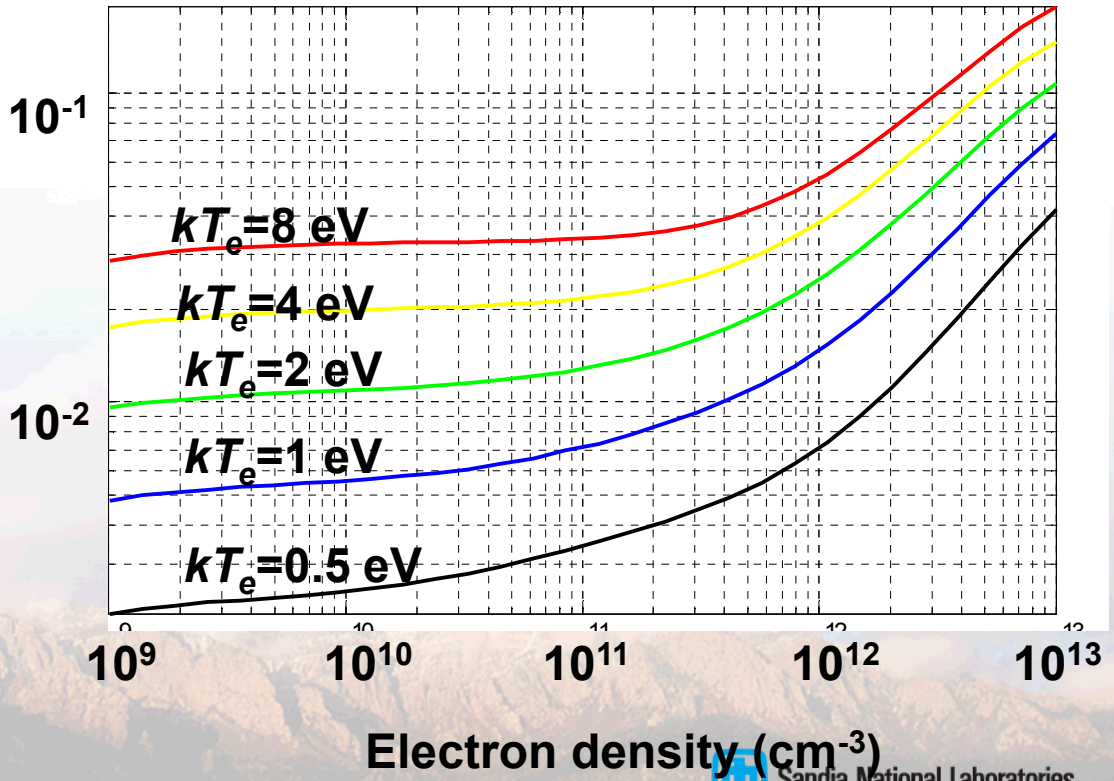

Key neutral physics

- **Discussion of key neutral-driven physics**
  - Collisional quenching
  - Redistribution to higher states

$$\frac{dN_j}{dt} = \sum_k \left[\sum_{i \neq j} K^a_{ikj} N_i - \sum_{i \neq j} K^a_{jki} N_j \right] N_k + \left[\sum_{i>j} A_{ij} N_i - \sum_{i<j} A^j_{ji} N_j \right]$$

Sandia National Laboratories

Neutral collisions can quench the excited state

- **Neutral collisions can impact the lifetime of the laser-excited state**

$$\frac{dN_j}{dt} = -A_{Effective} N_j \qquad \text{where} \qquad A_{Effective} = A_{Nominal} + K^a N_a$$

$$K^a \sim \pi a_0^2 \left(\frac{8kT_a}{M\pi} \right)^{1/2} p^2 \sim 10^{-11}\ \text{cm}^3/\text{s}$$

Quenched Population

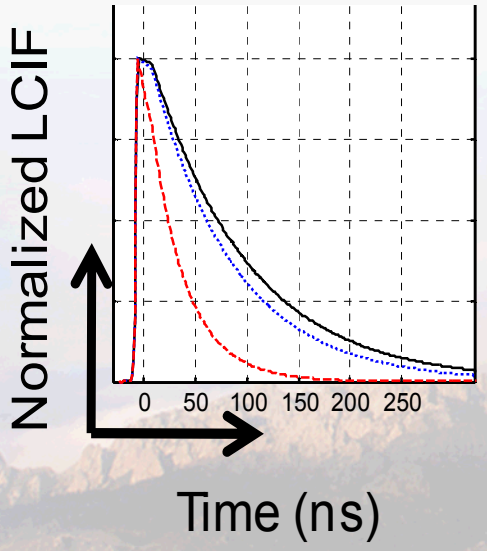

Lifetime of excited state

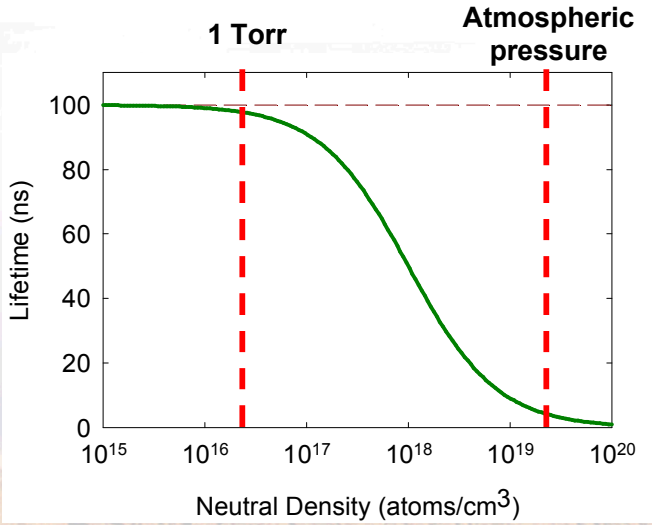

Nominal lifetime

$A_{Nom} = 10^7\ s^{-1}$
$K^a = 10^{-11}\ cm^3/s$

Sandia National Laboratories

Neutral collisions can drive up-hill transitions

- **Proximity (energetically) of states means neutrals can transfer excited population to 3^3D**
  - Energy spacing between states is 0.067 eV ~ 780 K

Amount of 3^3D produced from 3^3P

$$\Delta N_{Electrons} \sim K^{e}_{P->D} n_e \Delta N_P \Delta t \quad \text{and} \quad \Delta N_{Neutrals} \sim K^{N}_{P->D} n_0 \Delta N_P \Delta t$$

Bound determined by setting the two equal

$$\frac{\Delta N_{Electrons}}{\Delta N_{Neutrals}} \sim \frac{K^{e}_{P->D} n_e}{K^{N}_{P->D} n_0} \sim 1$$

Solve for n_e

$$n_e \sim \frac{K^{N}_{P->D}}{K^{e}_{P->D}} n_0 \sim \frac{10^{-12}}{10^{-5}} n_0$$

Pressure dependent density bound

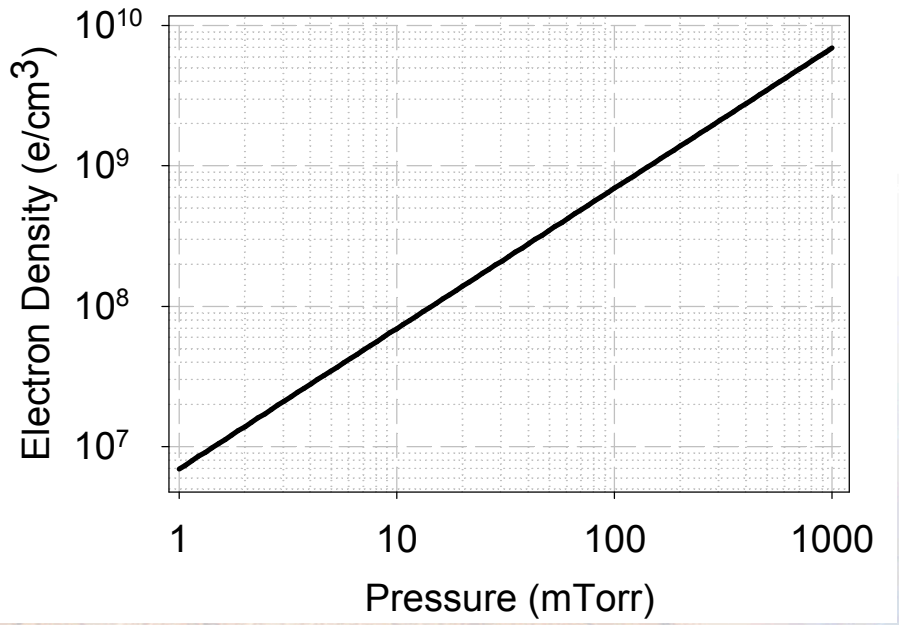

Lower limit on electron density scales with pressure (and temperature) of neutral background

R. Denkelmann, S. Freund and S. Maurmann, Contrib. Plasma Phys. **40**, 91 (2000).

Laser-collision induced fluorescence provides measure of electron density and "temperature"

- **Motivation: What is the density? What is the temperature? Where and When?**
  - More traditional probe techniques may couple and perturb
  - Optically passive techniques are line-of-sight limited
  - Optically active-techniques such as Thomson scattering pose their own set of challenges

- **In this presentation**
  - Part I: Laser-collision induced fluorescence (LCIF) primer
    - Collisional-radiative model used to predict LCIF
    - Physics that governs LCIF
  - **Part II: Implement and benchmark technique**
    - **Experimental setup**
    - **Time evolution of LCIF and time integrated LCIF**
  - Part III: Applications of LCIF:
    - Dynamic and structured plasmas
  - Part IV: Future directions and concluding comments
    - Investigate argon

Sandia National Laboratories

Part II: LCIF implementation and benchmark

- **Implement and benchmark technique**
  - Experimental considerations
  - Benchmarking LCIF - compare observations with anticipated trends

Experimental setup

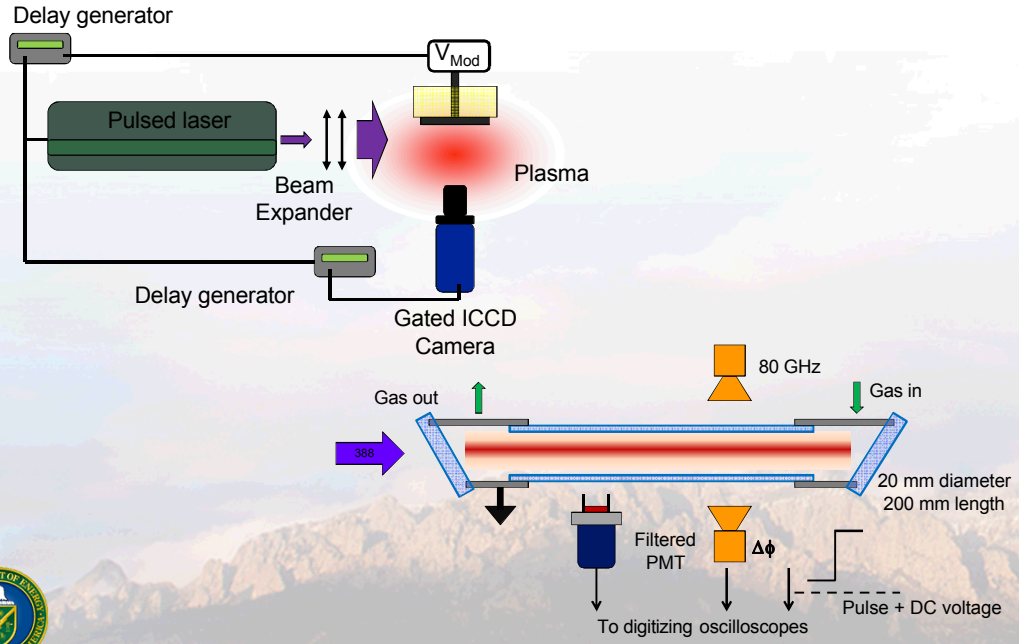

Benchmark LCIF

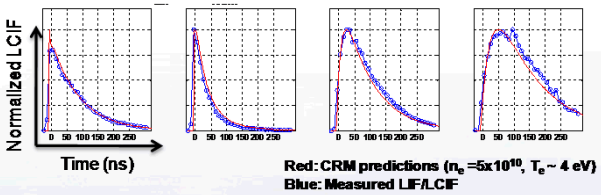

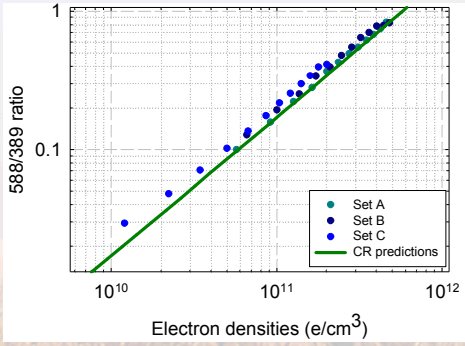

Experimental implementation of the LCIF is realized

- **Nanosecond pulsed laser used for excitation**
  - < 10 ns FWHM, < 0.1 cm^{-1} line width
- **Timing of experiment controlled by delay generators**
  - Move experiment and imaging with respect to firing of the laser
- **Image LCIF with gated-intensified CCD**
  - Narrow (~ 1 nm FWHM) interference filters centered on lines of interest
- **Take two images per transition considered**
  - Total emission and plasma induced emission (PIE) - subtract the two

Optical setup

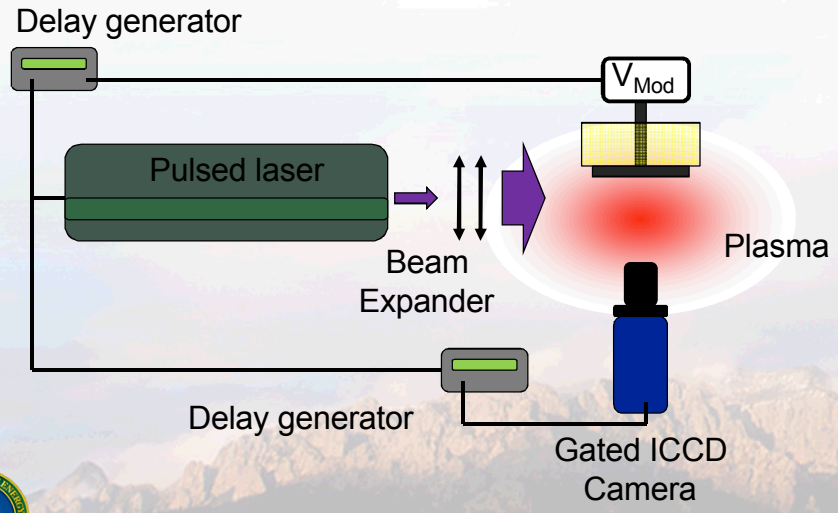

Timing sequence

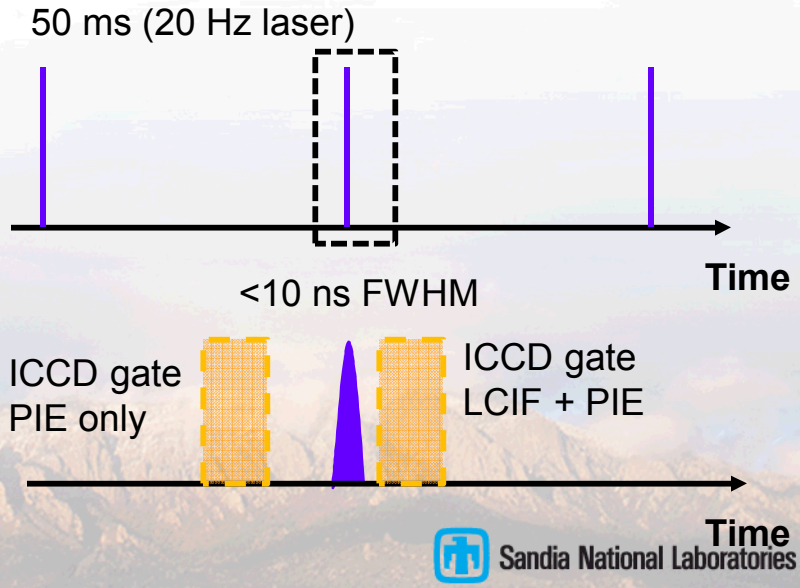

Laser-collision induced fluorescence is obtained by observing light emitted after excitation

- **The light emitted from an excited state is proportional to the population of that state, and how likely it will radiate from that state.**
  - Differences in the A coefficients will impact how "bright" the transition appears

$$Photons\ emitted \sim A_{jk} \times \Delta N_j \times \Delta t$$

- **Photon detection is dependent on the efficiency of the detection system**
  - Identification and calibration of these factors is required if intensities are utilized

$$Photons\ detected \sim \varepsilon_{System} \times Photons\ emitted$$

$$\varepsilon_{System} \sim \varepsilon_{Detector}\varepsilon_{Collection}\varepsilon_{Plasma}\cdots$$

Sandia National Laboratories

Pulsed positive column is utilized to benchmark LCIF technique

- **Pulse discharge currents generate broad density range**
  - ~ 10 Microseconds,
- **Compute drift velocities and extract electron temperatures**
  - Use published drift parameters

Positive column

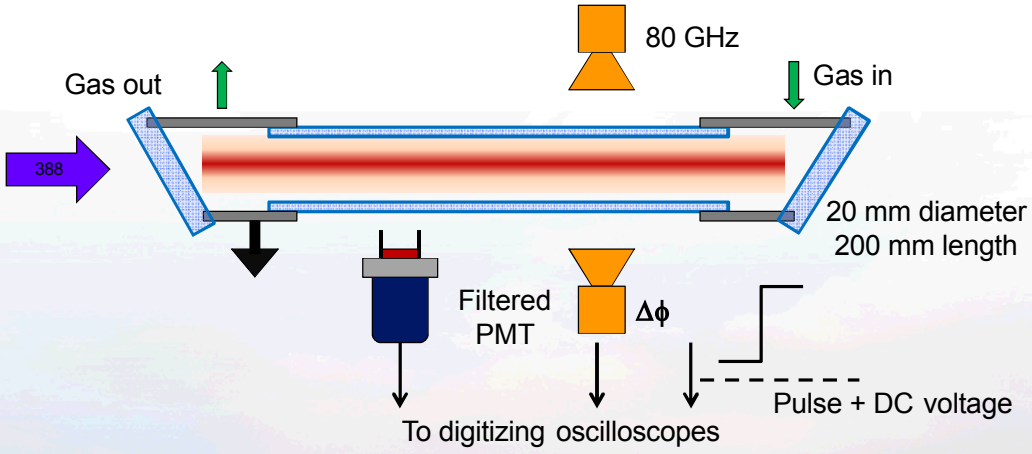

Helium drift parameters

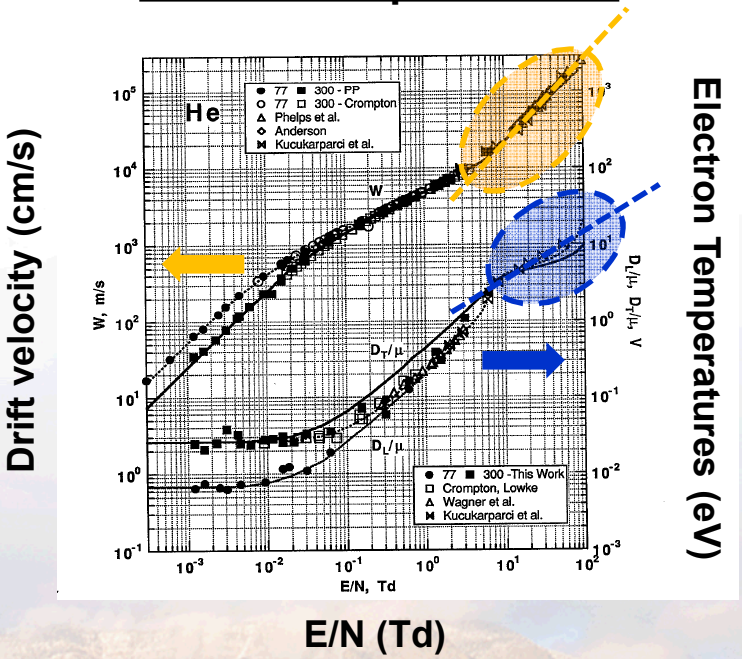

J. L. Pack, R. E. Voshall, A.V. Phelps and L. E. Kline, J. Appl. Phys. V71, p5363 (1992)

Sandia National Laboratories

ELECTRON DENSITIES ARE CHARACTARIZED UTILIZING MICROWAVE BASED TECHNIQUES

- **Earlier diagnostics utilized microwave interferometer to measure electron densities.**
  - Transmissivity (refraction) likely lead to errors in densities.
- **Recent diagnostics are using a microwave resonant cavity to interrogate plasma densities.**
  - Analytic solutions usable for most of parameter space of interest.
  - Full EM solve for higher densities (P. Miller).

Microwave Interferometer

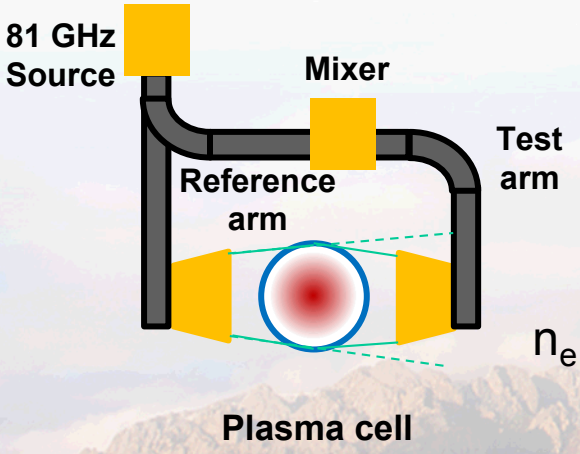

$n_e \sim \Delta\phi$

Microwave Resonant Cavity

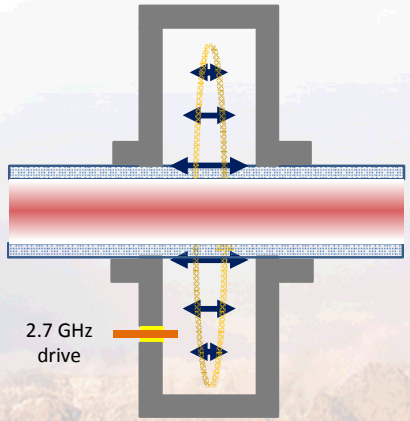

$n_e \sim \Delta f/f_0$

First steps: Verify time resolved LCIF to test CRM

- **Excite the 23S – 33P transition @ 389 nm**
  - Monitor LIF back to 2^3S
  - Monitor LCIF from 3^3D and 4^3D
- **Compare measured results to simulated results**

Key transitions

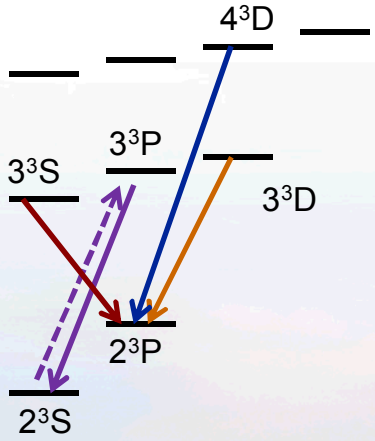

Representative results

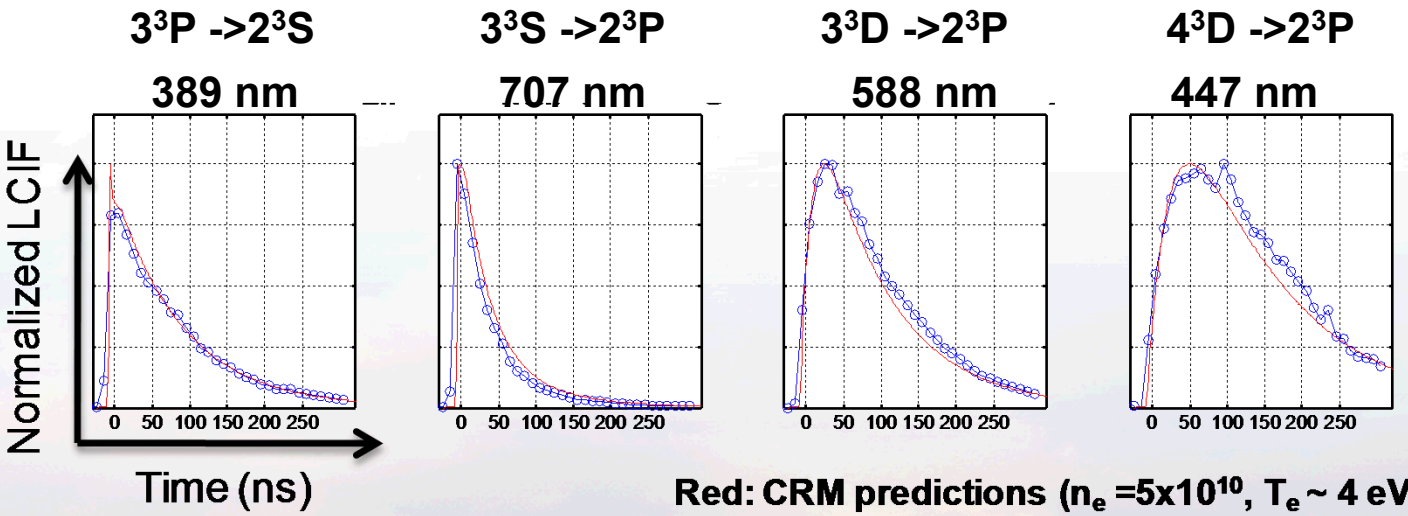

Red: CRM predictions (n_e =5x10^{10}, T_e ~ 4 eV)
Blue: Measured LIF/LCIF

[588]/[389] ratio exhibits linearity over nearly two orders of magnitude

- **Better yet, measured ratios agree reasonably well with computed ratios**
  - Slightly higher, and some deviation at low density
- **Examined trends at different times during the current pulse**
  - Anticipate different temperatures as column is established

Waveforms during excitation

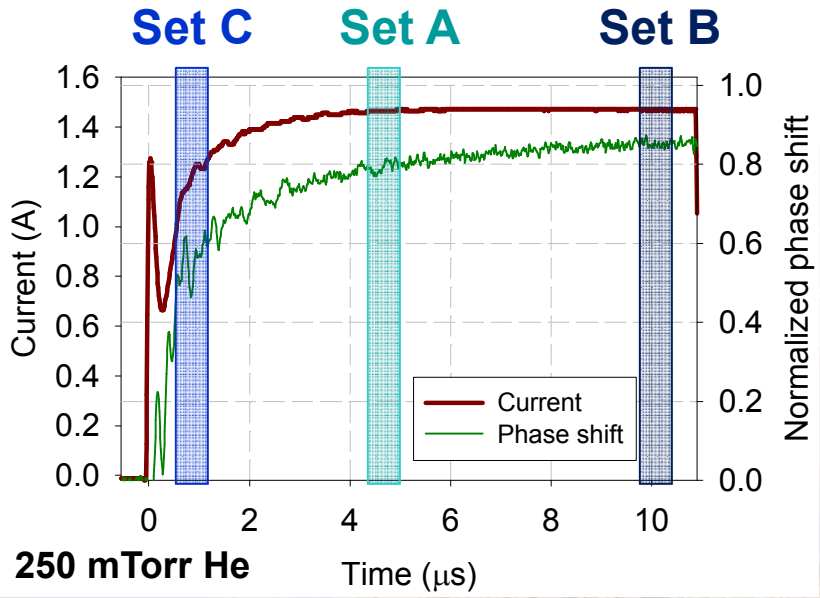

Density dependent ratio trends

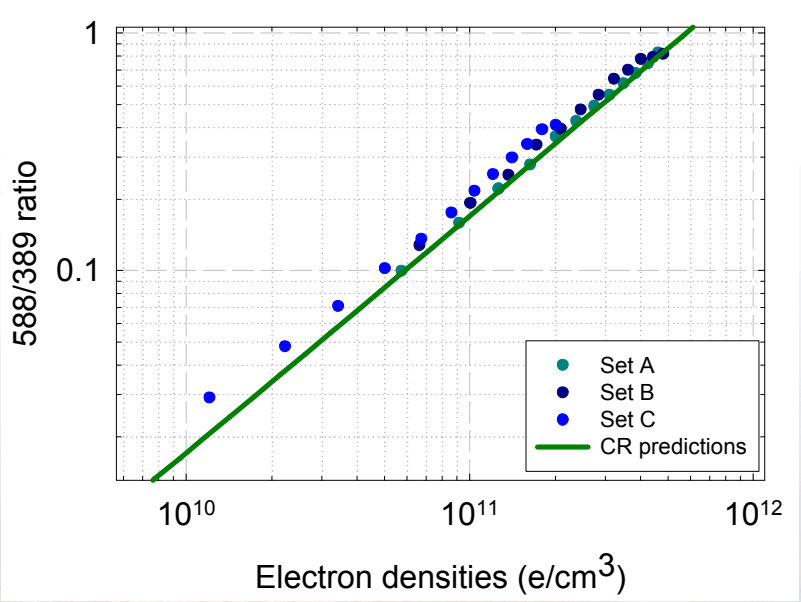

Density measurements obtained at different times essentially overlay each other

[447]/[588] ratio captures trends but misses absolutes

- **Anticipated T_e trends are observed**
  - High temperature at start, low temperatures later on
- **Measure T_e trends mimic computed trends**
  - Discrepancy in absolute values are apparent

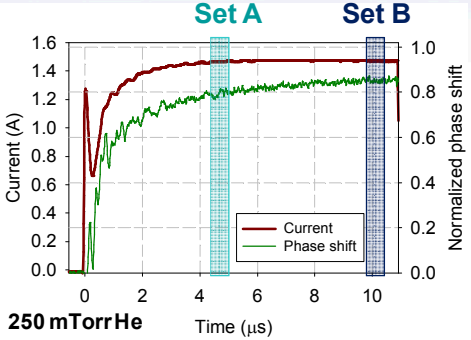

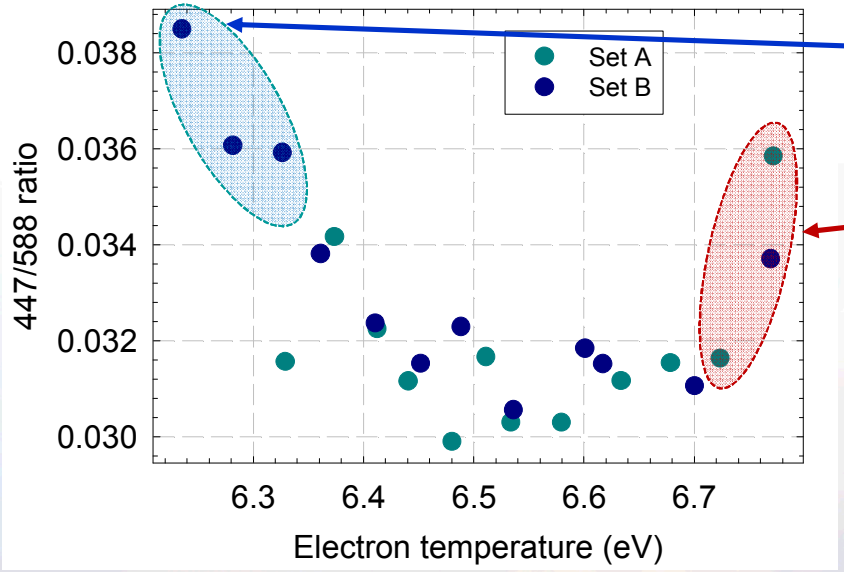

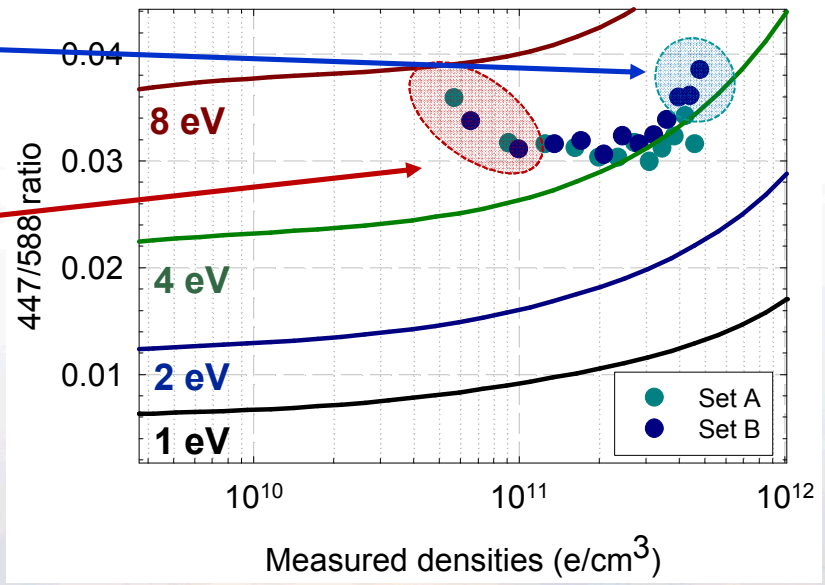

Uncertainties in rates, EEDF and/or interpolation of T_e from drift parameters should impact absolute values

DOUPLE PULSE SETUP ENABLES CONTROL OVER DENSITY AND "TEMPERATURE"

- **Double-pulse technique is utilized to gain more control over the "effective" electron energy.**
  - First pulse generates the host plasma.
  - Second pulse drives current through the plasma and tunes E/N.

Excitation Scheme

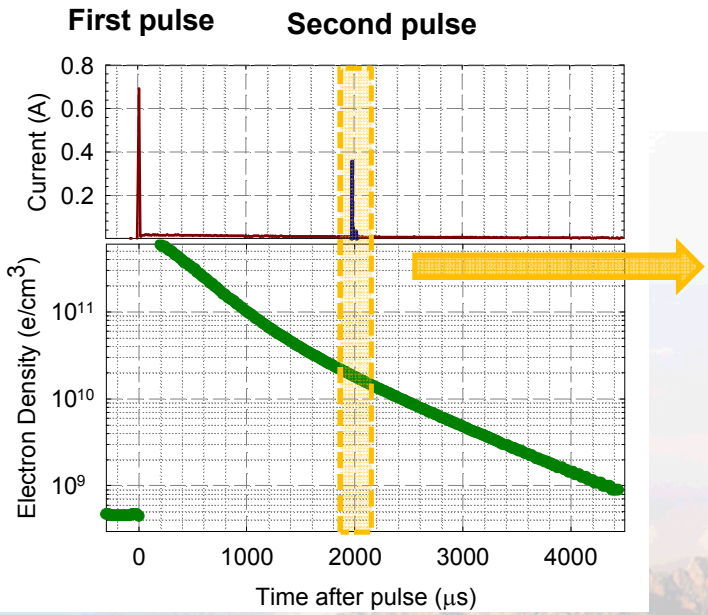

Plasma response to second pulse

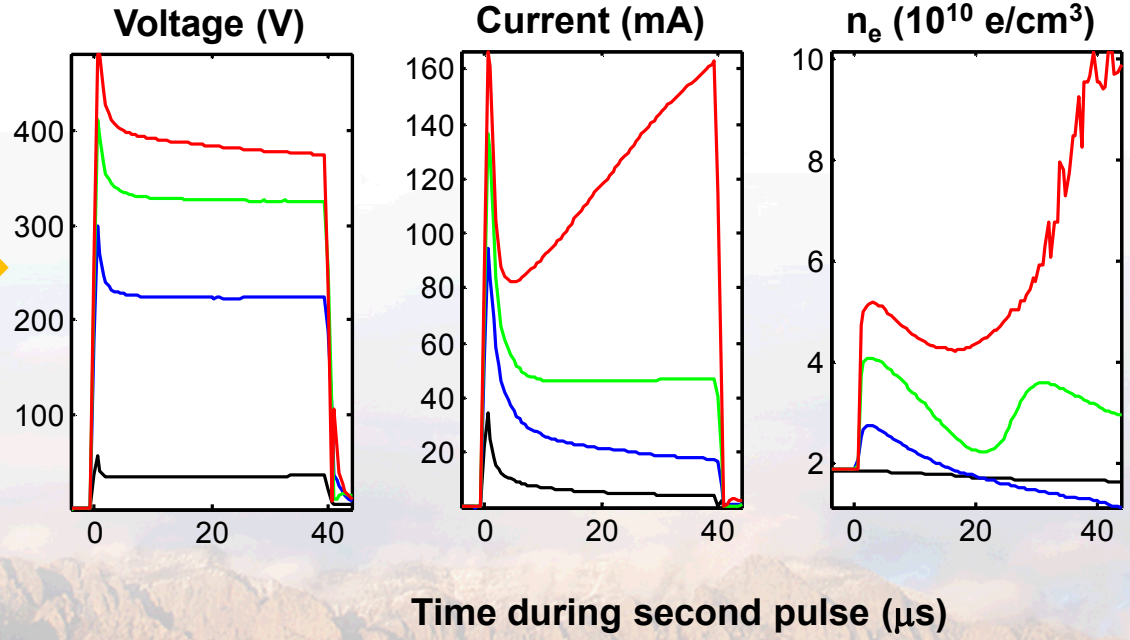

E/N IS MANIPULATED WITH THE SECOND VOLTAGE PULSE

- **Published drift parameters are utilized to correlate drift velocities to E/N**
  - Excitation and ionization compliments analysis.
- **Applied voltage across the column "tunes" E/N.**
  - E/N spans ~ 1 Td -> 50 Td.

Time averaged parameters

5 μs average, 10 μs after pulse is applied

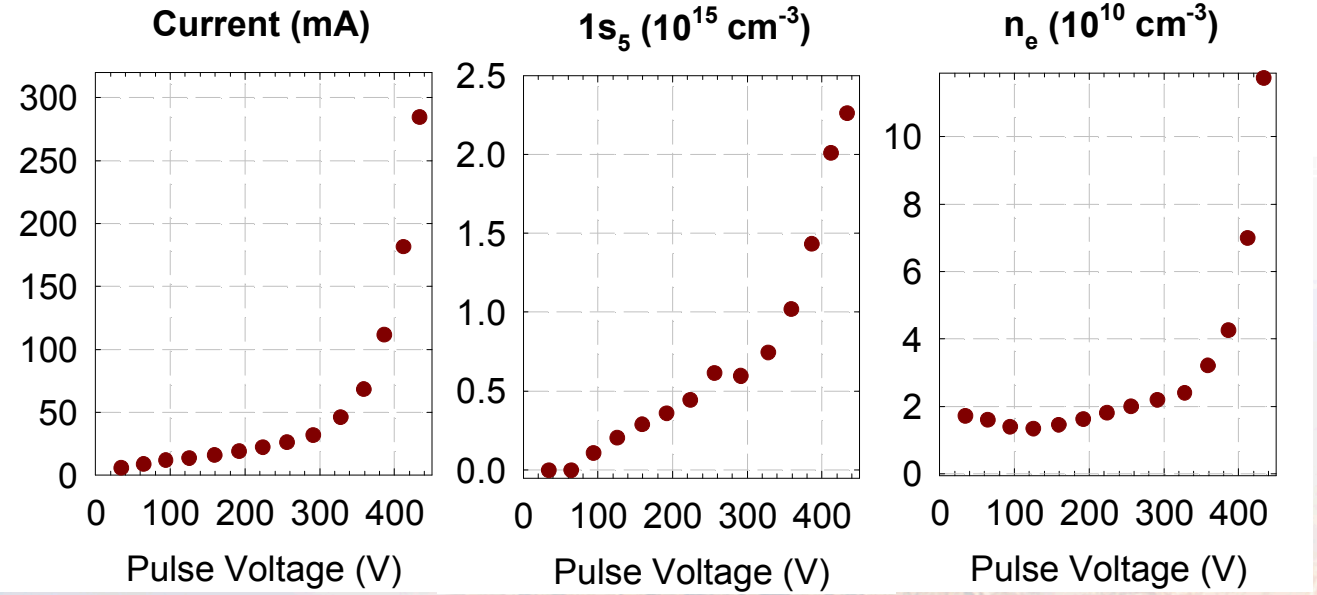

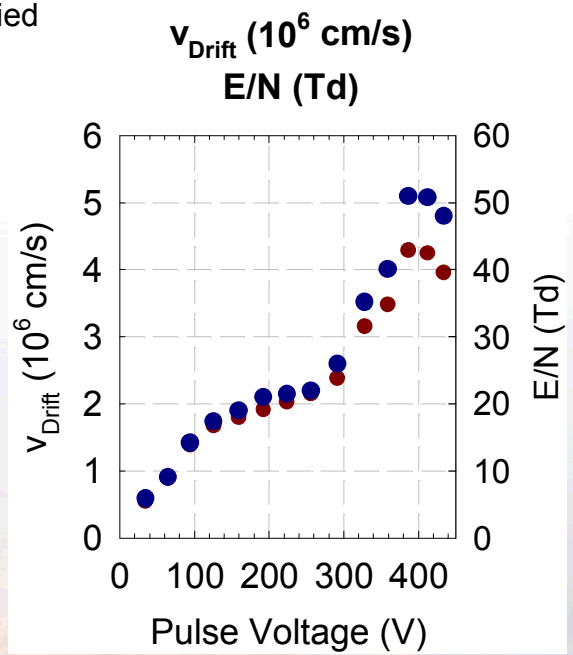

Other spectroscopic pathways can be considered for LCIF measurements

- **Lower base density of 2^3P advantageous, when radiation trapping is an issue**
  - Lose the nice "temperature free" 3^3P -> 3^3D transition
  - Spectrally dense - many transitions ~ 400 nm
  - Rates not as well known….

Excitation scheme

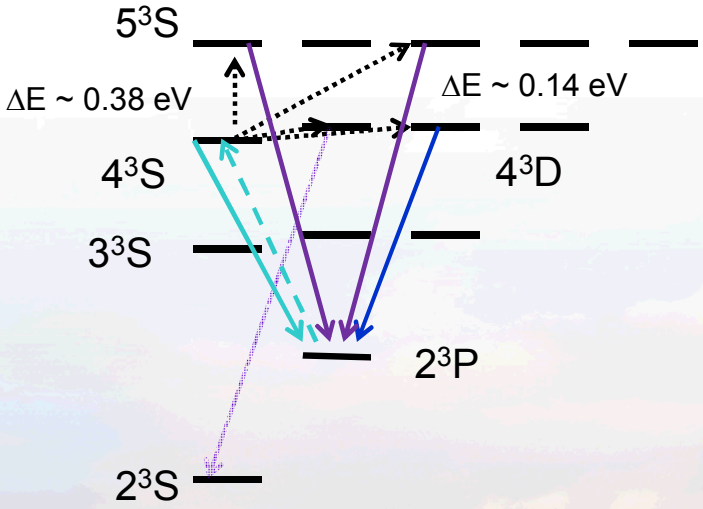

Key rates utilized in "CRM"

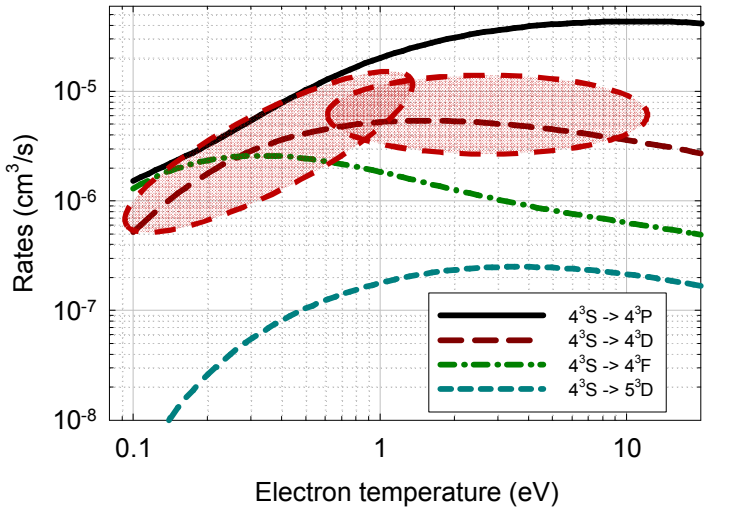

[1] Yu. Ralchenko, R. K. Janev, T. Kato, D. V. Fursa, I. Bray, F. J. De Heer, Atomic Data and Nuclear Data Tables **94**, 603 (2008).

2^3P excitation pathway is also benchmarked

- **Utilize simple set of coupled equations to compute evolution of the system**
  - Not self consistent, but sidesteps many unknowns
  - Rely on functional forms of excitation cross sections[1]

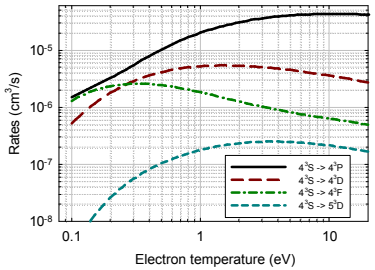

Spectroscopic pathway

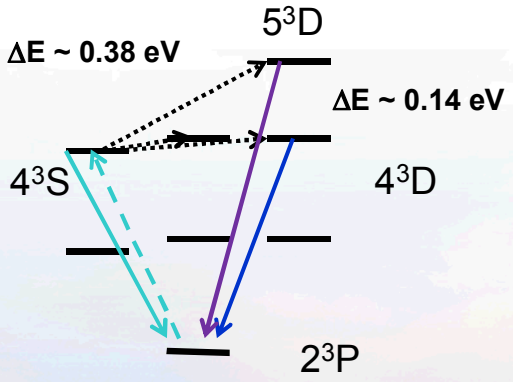

Key Scaling Trends

Electron density

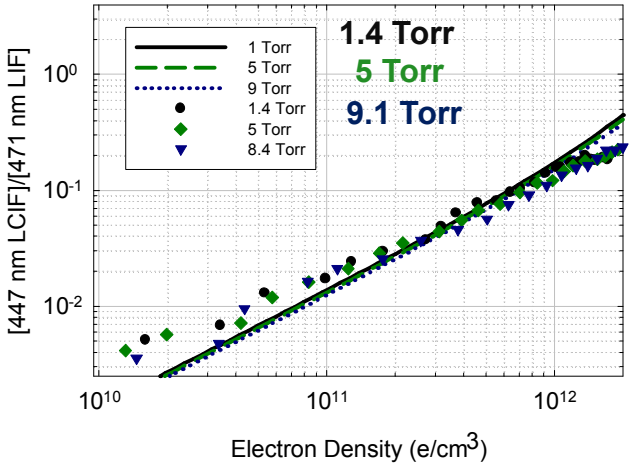

"Electron Temperature"

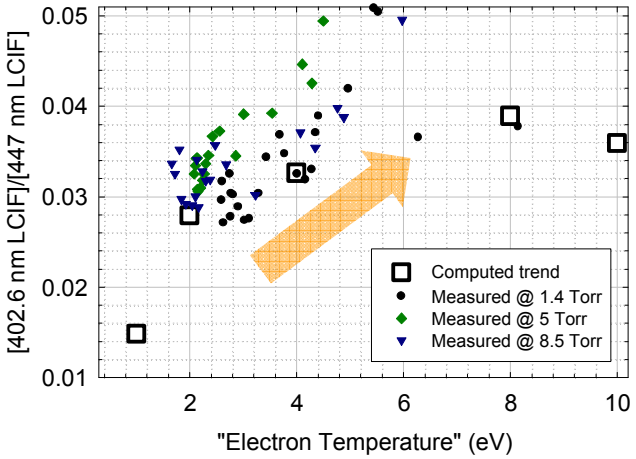

Electron density trends are independent of electron temperature and gas pressure

[1] Yu. Ralchenko, R. K. Janev, T. Kato, D. V. Fursa, I. Bray, F. J. De Heer, Atomic Data and Nuclear Data Tables **94**, 603 (2008).

Complexity of many atomic systems makes LCIF "challenging"

- **Complex atomic structure**

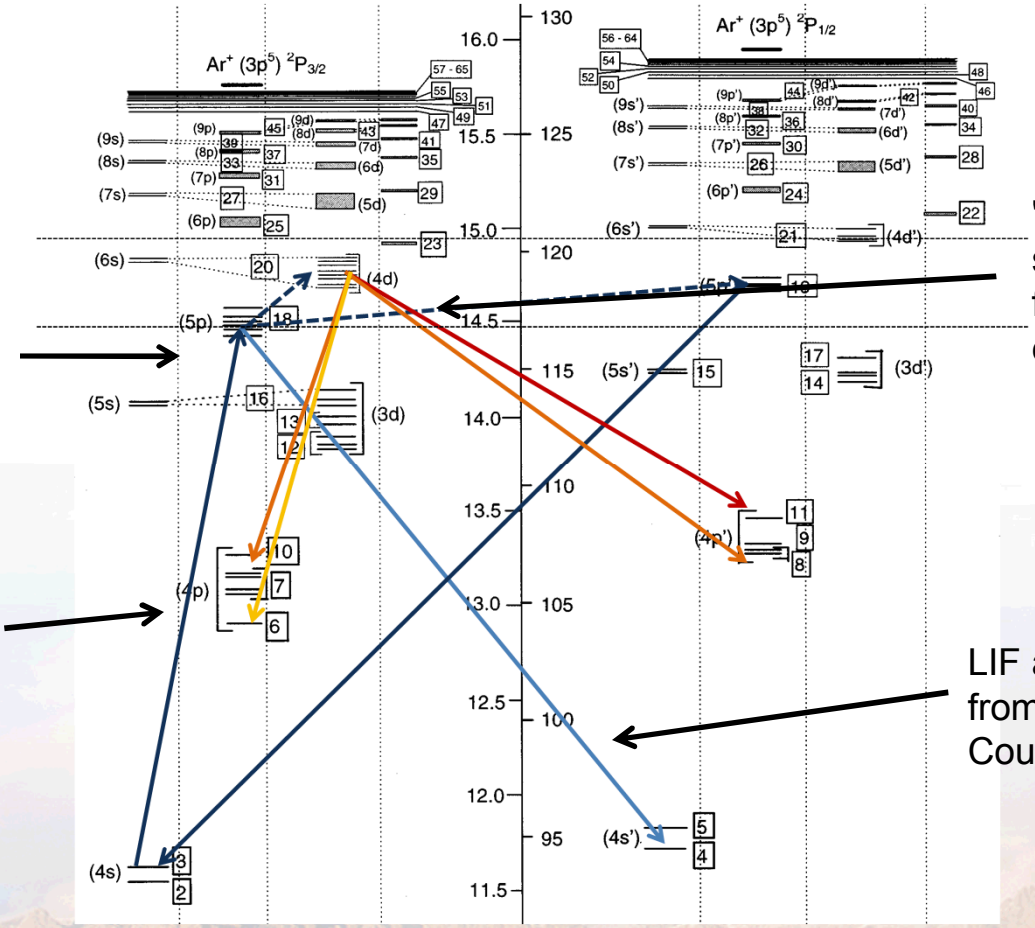

Targeting lowest lying $3p_{10}$ state

Not pursuing radiation trapped 2p states

"Orange" LCIF from 4d states well separated from "red" lines emanating from 2p states

LIF at 470.2 is well isolated from other transitions Coupled to $1s_2$ state

Taken from Bogearts et. al, J. Appl. Phys. **84**, 121, 1998

Cross sections and rates not well known for electronic driven processes from 3p to higher states

METHODS ARE BEING REFINED AND NEW DIAGNOSTICS ARE BEING IMPLEMENTED

- Argon laser collision induced fluorescence is being developed
  - Brandon Weatherford was developing (Hired to L3 Communications).
- Non-unity scaling with density have hindered completion.
  - Errors in density measurement, impact of electron temperature or spectral contamination are likely sources of scaling.

Excitation scheme

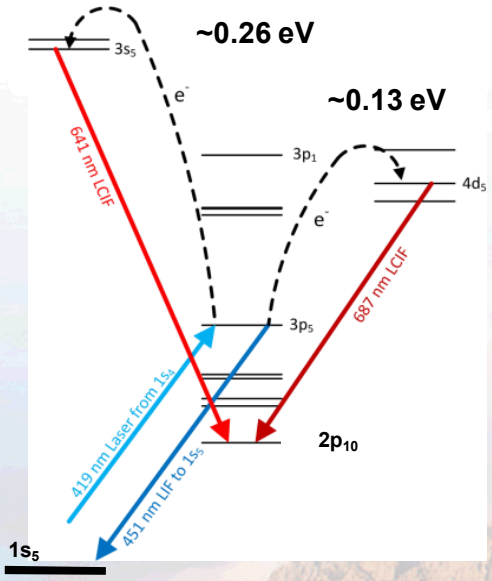

Argon LCIF

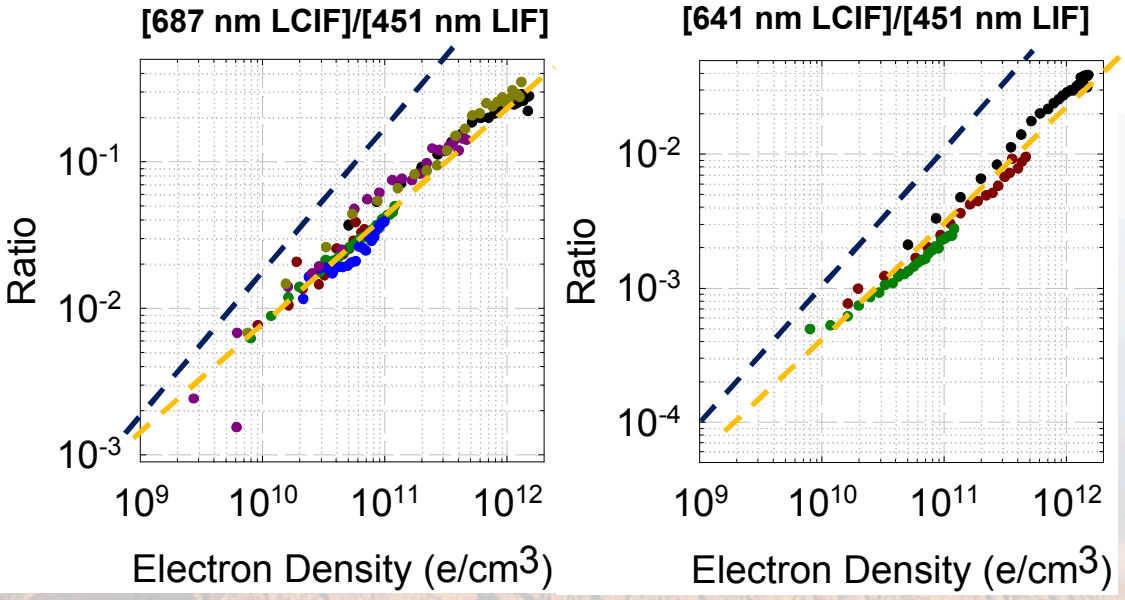

Laser-collision induced fluorescence provides measure of electron density and "temperature"

- **Motivation: What is the density? What is the temperature? Where and When?**
  - More traditional probe techniques may couple and perturb
  - Optically passive techniques are line-of-sight limited
  - Optically active-techniques such as Thomson scattering pose their own set of challenges

- **In this presentation**
  - **Part I: Laser-collision induced fluorescence (LCIF) primer**
    - **Collisional-radiative model used to predict LCIF**
    - **Physics that governs LCIF**
  - Part II: Implement and benchmark technique
    - Experimental setup
    - Time evolution of LCIF and time integrated LCIF
  - **Part III: Applications of LCIF:**
    - **Dynamic and structured plasmas**
  - Part IV: Future directions and concluding comments
    - Investigate argon

Sandia National Laboratories

Part III: Applications of LCIF

- **Applications of LCIF**
  - Studying dynamic and structured plasmas

Emphasize structure and evolution of the plasma being studied

Experiment designed for flexibility

- **Time modulated rf plasma**
  - Generate metastable "seed " to prepare for transient measurements
- **Segmented electrodes**
  - Positive and or negative polarity pulses
- **Computer controlled delays**
  - Time step across event of interest

Setup

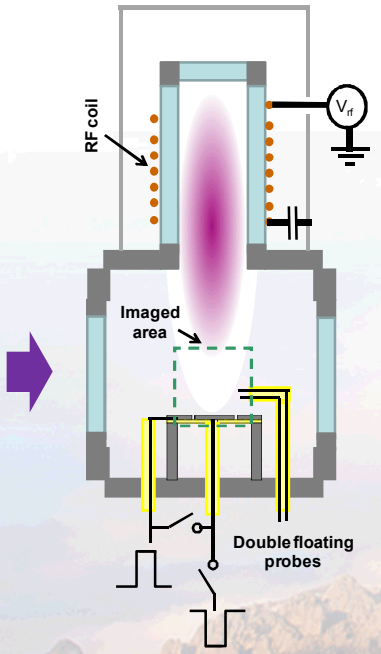

Timing sequence

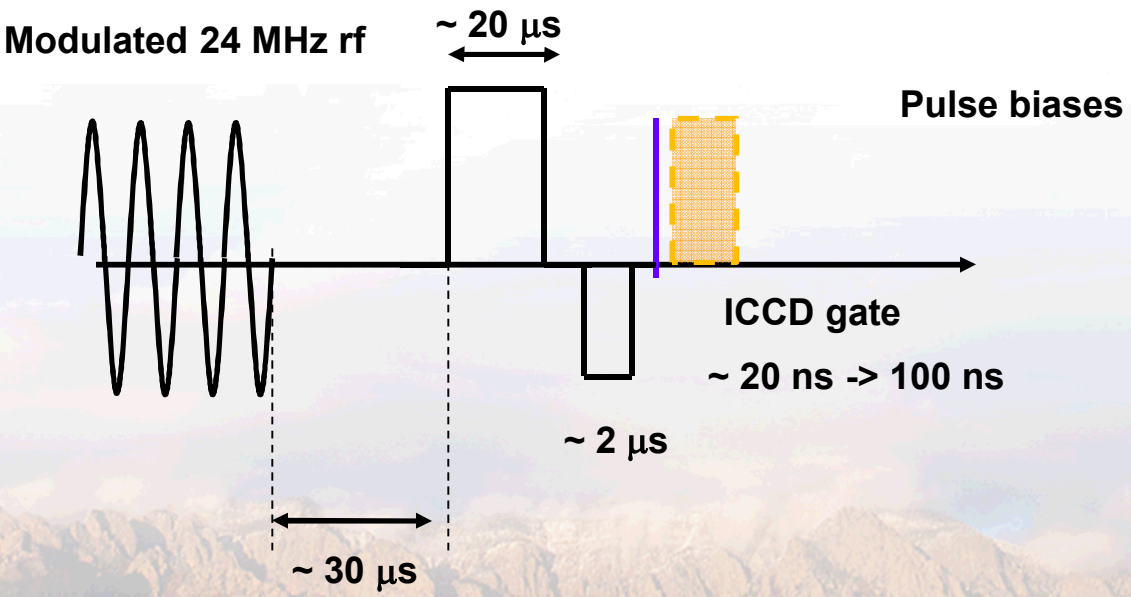

Examine phenomena on different spatial and temporal scales

LCIF is utilized to study transient plasma

- **Trends analyzed with CR model**
  - Produce n_e, T_e as functions of time

Setup and behavior

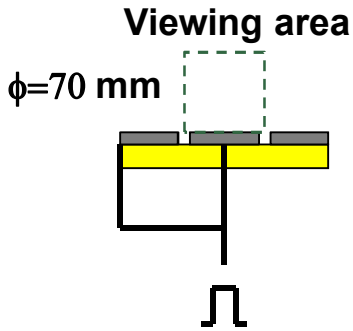

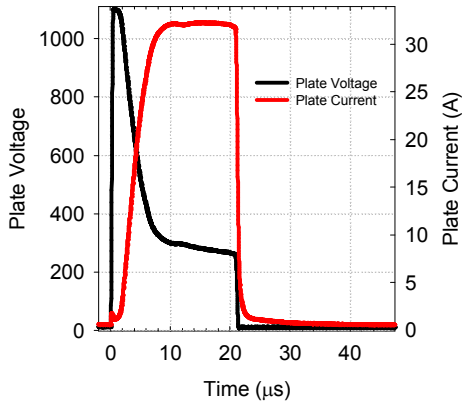

LCIF Trends

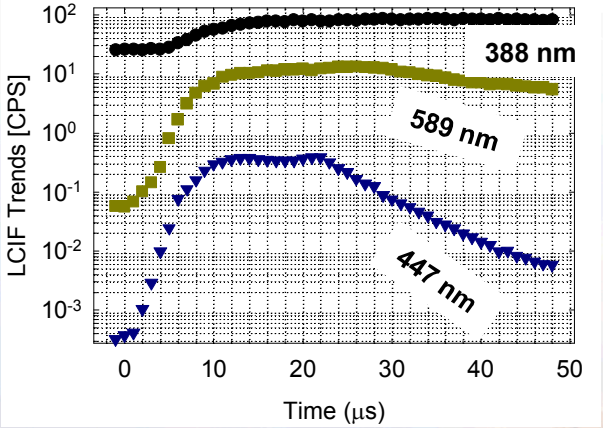

LCIF Ratios

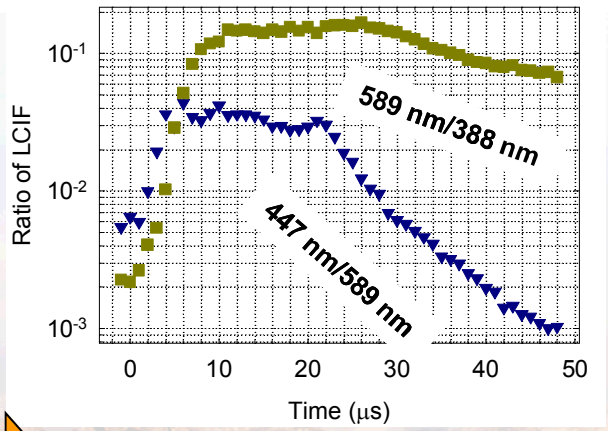

Densities and temperatures

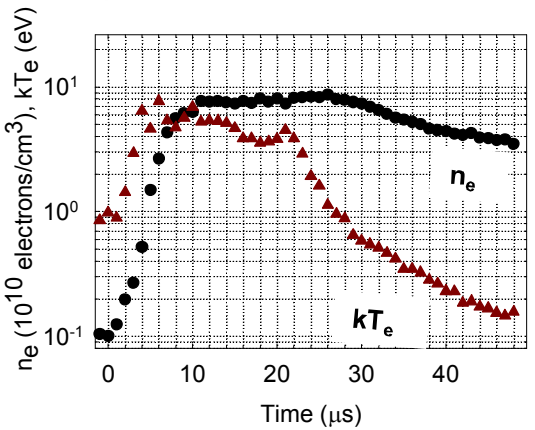

LCIF captures the evolution of transient plasma

Sandia National Laboratories

Demonstration of LCIF technique: 2D-ion sheath formation

- **Examine evolution and structure of ion sheath**
  - - 1 kV bias applied to inner electrode, 50 μs into afterglow (low n_e, low kT_e)
  - 20 ns snapshots of LCIF, 30 ns steps

Setup

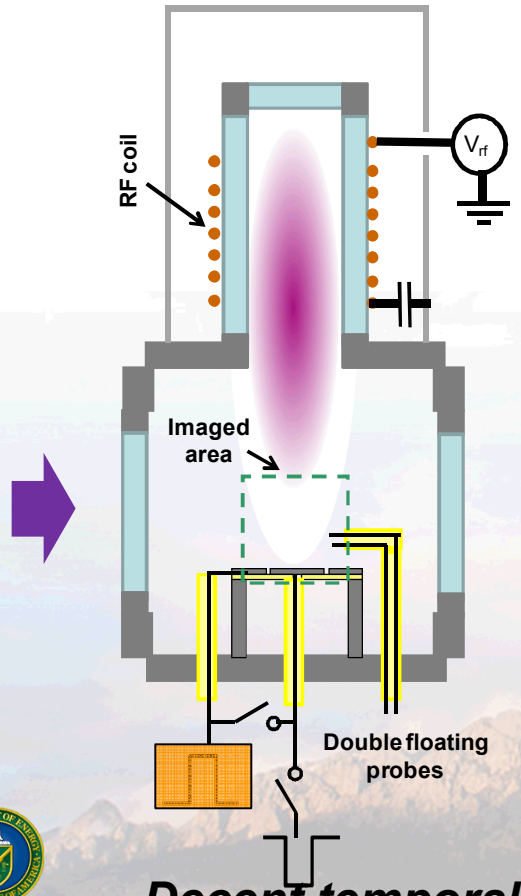

Data

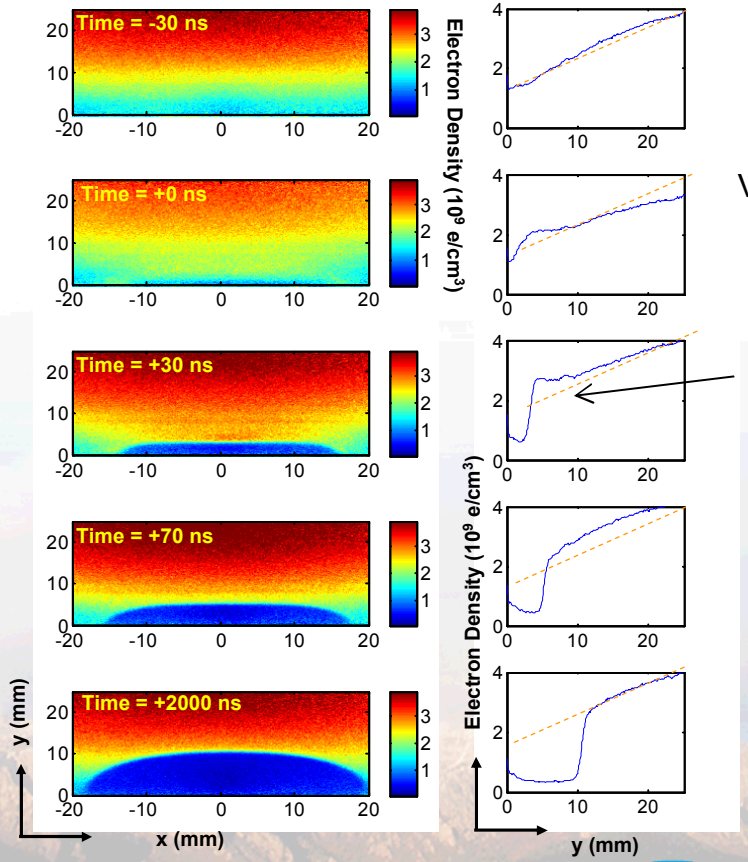

Initial structure

Voltage applied

"Matrix" sheath

Sheath evolving

Final sheath structure

Decent temporal and spatial resolution demonstrated

Sandia National Laboratories

Interesting structure observed in the sheath

- **LCIF signal observed deep in the sheath**
  - Some caused by neutrals, but not all

2D Images

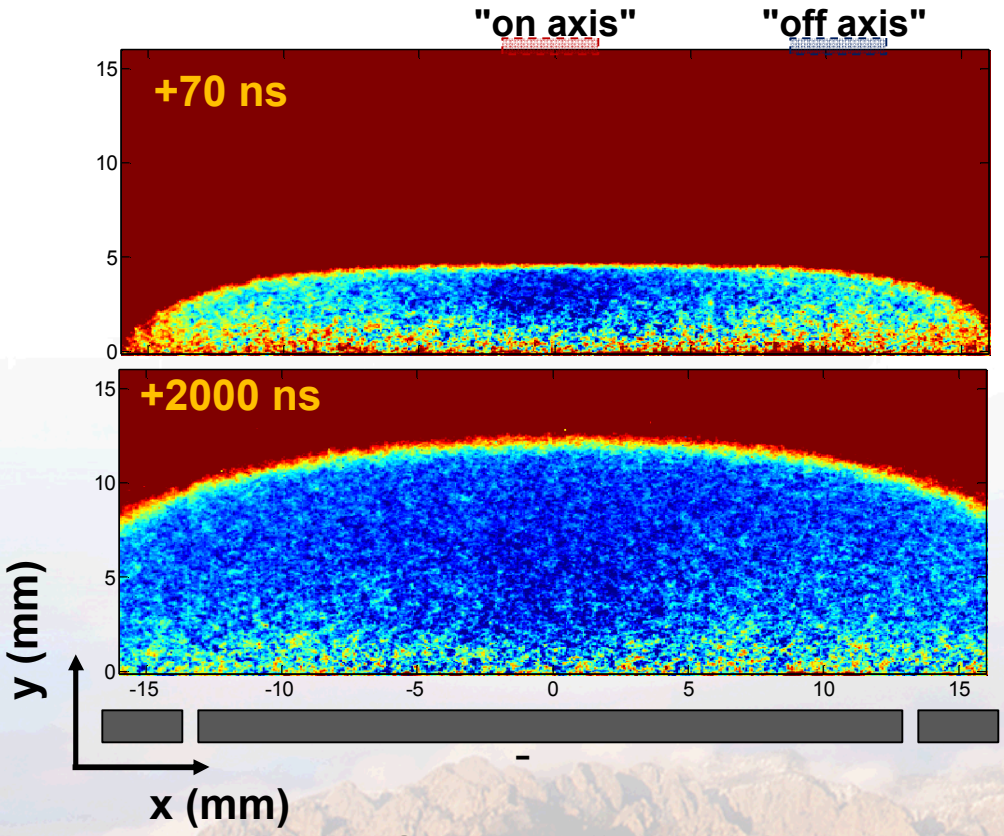

Profiles

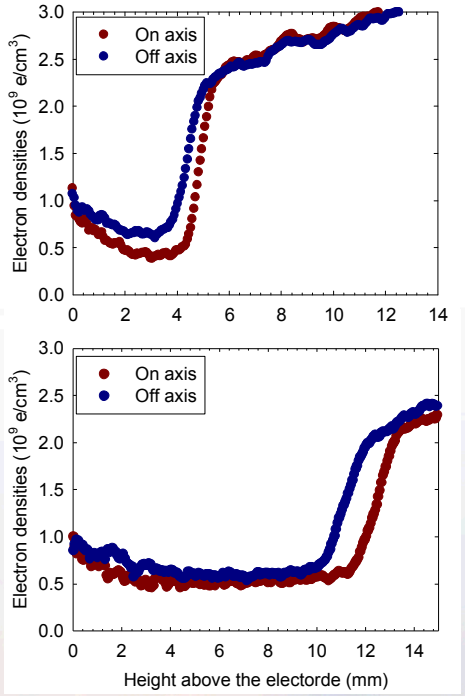

Signal deep in the sheath caused by electrons emitted from the electrode

Transient anodic double layer observed after pulsed excitation

- **Closer analysis of initial plasma distribution**
  - Use smaller (25 mm) diameter electrode, 100 mTorr afterglow

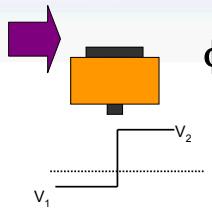

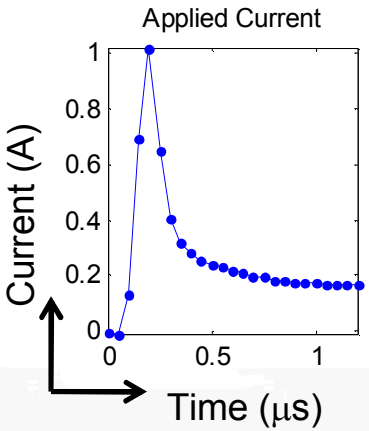

Earlier times

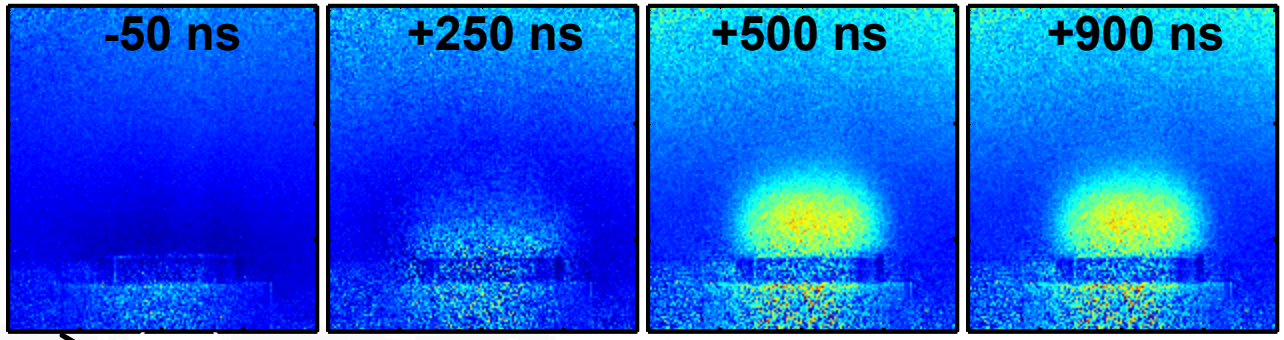

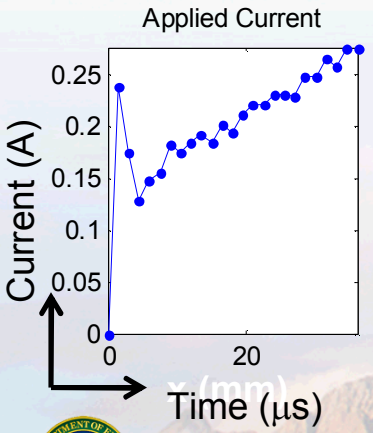

Later times

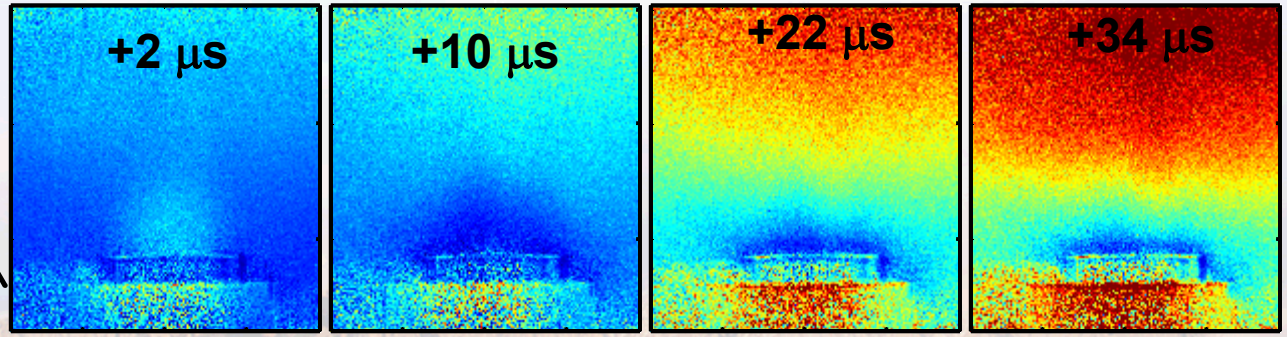

Structure undergoes inversion after stagnation

Higher energy electrons observed around edge of anode plasma

- **Temperature measurements made for +900 ns case**
  - Challenging measurement because of low level signals

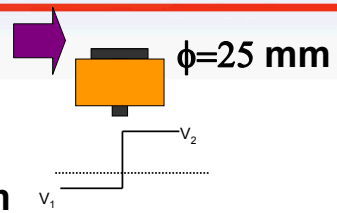

LCIF Data

388 nm

589 nm

447 nm

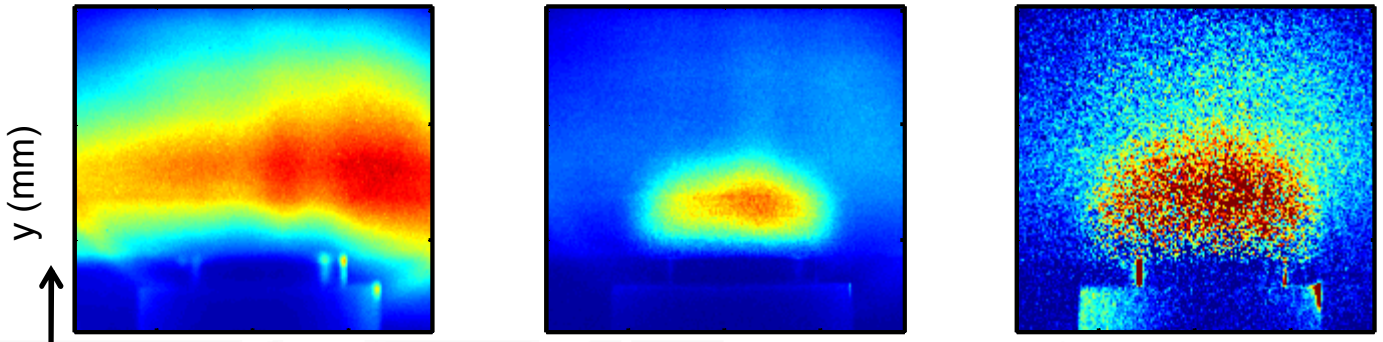

Analysis

Electron Densities

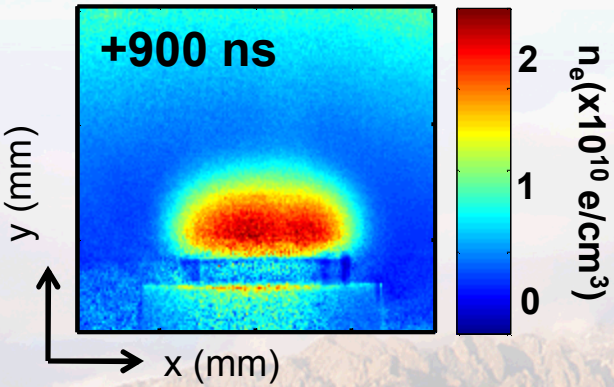

Electron Temperatures

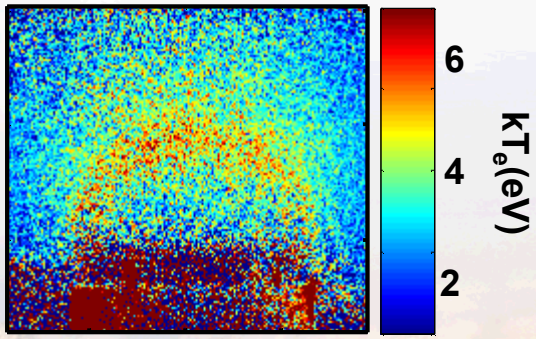

"Anodic Fireball"

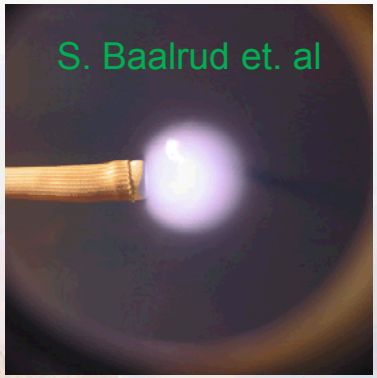

Electrons energized by localized electric fields supporting double layer

S. D. Baalrud , B. Longmier and N Hershkowitz, Plasma sourc. Sci. Technol. 18 035002 (2009)

Double layer more pronounced in ECR based plasma cathodes

- **NASA driven research interested in electron sources for propulsion**
  - Understand limitations on current extraction
- **Host Brandon Weatherford (U. Mich.) to implement LCIF**
  - Examine coupling of between plasma generation and electron extraction

Setup

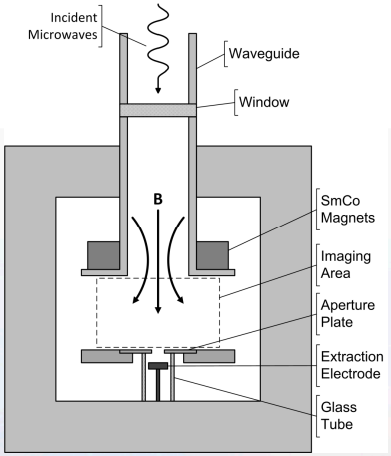

"Full color" picture

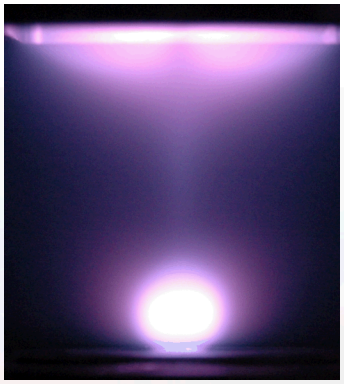

Density

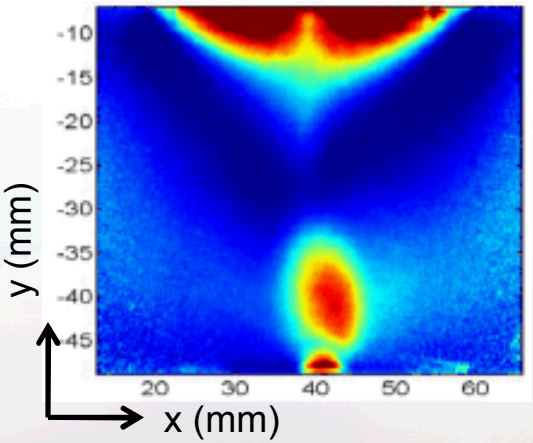

Temperature

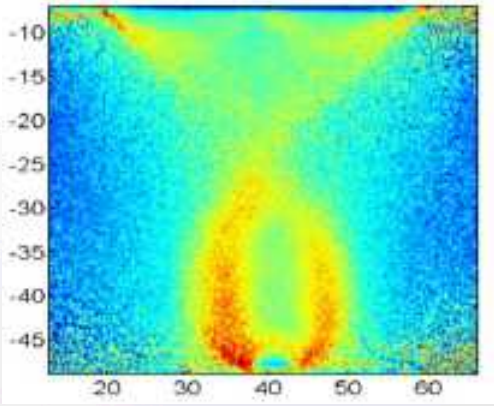

Multi-structure plasma formed by electron-extracting electrode...
... quite difficult to probe with more conventional means!

Sandia National Laboratories

LASER DIAGNOSTICS DEVELOPED IN PSC INTERROGATES MAGNITIZED PLASMA

- **Plasma transport in magnetized plasma is important to understand but challenging to assess**
  - Magnetic configuration dictates particle balance in the plasma
- **Hosted Aimee Hubble (Ph.D. candidate w/ John Foster, U. Michigan) to address fundamental questions about electron loss**
  - Segmented, magnetized anode to quantify plasma confinement
  - LCIF to interrogate electron densities and measure leakage widths

Measured electron densities

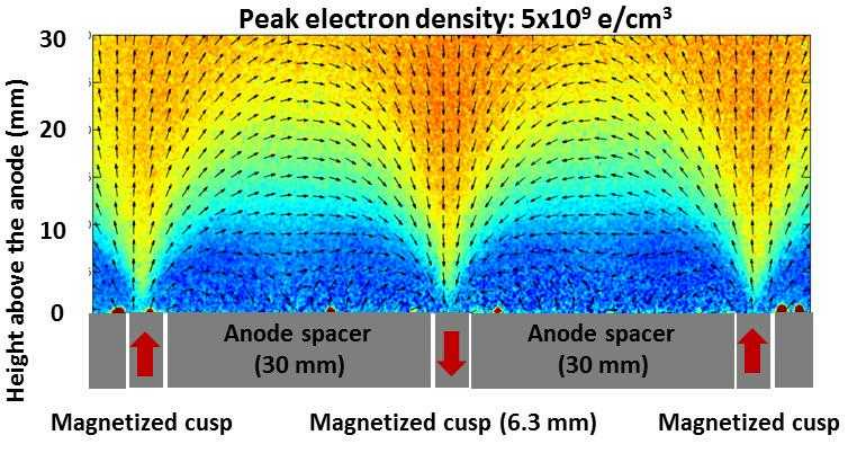

Electron leakage widths

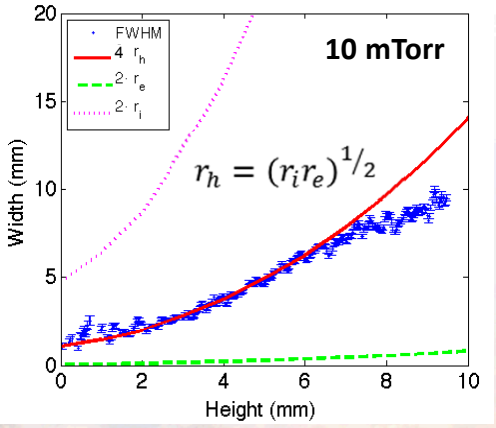

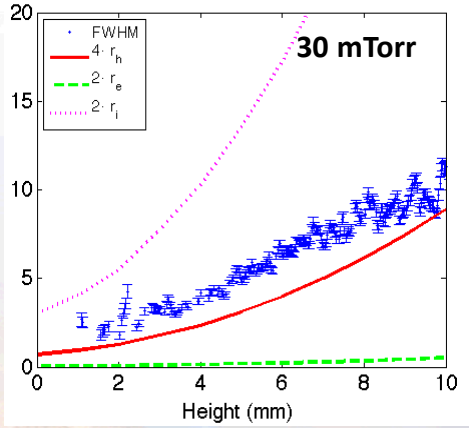

- **Measured electron densities, temperatures and magnetic fields are used to compute leak widths**

PLASMA TRANSPORT IS REGULATED BY THE ANODE POTENTIAL

- Transient plasma enables access to different current collecting conditions
  - Dial in potential drop between the anode and plasma
- Confinement degrades as electrode potential approaches plasma potential
  - Ion flux carries electrons across the magnetic fields

Anode drive

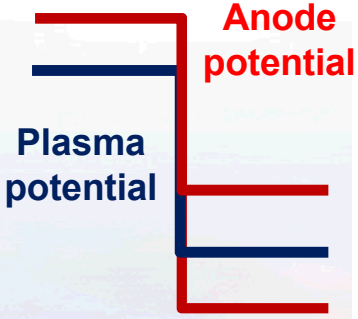

Measured electron densities

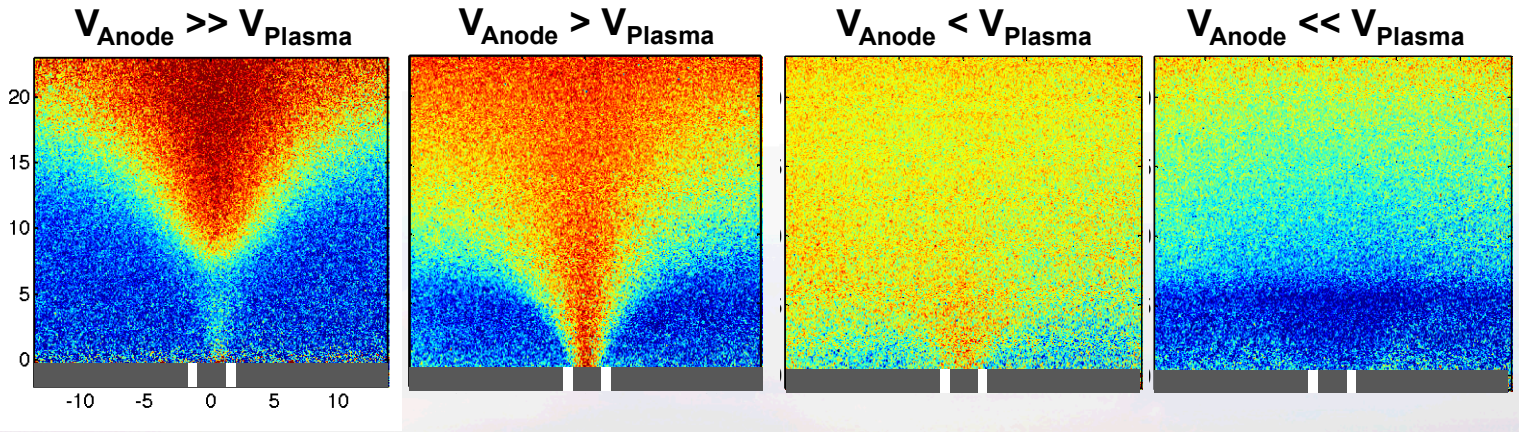

Sandia National Laboratories

Concluding remarks and future directions

- **LCIF technique demonstrated in 2D**
  - Free of “line of sight” constraints
  - Good spatial resolution – limited by optical collection
  - Decent temporal resolution – limited by ICCD gate times & tolerable signals

- **Caution required for proper implementation of the technique**
  - Uncertainties about rates – Absolute bounds on measurements
  - Proper choice of model – Capture the required physics

- **Technique should be extendable over broad parameter space**
  - Higher pressures – neutral collisions
  - Smaller dimensions – scattering and access
  - Other atomic systems

This work was supported by the Department of Energy Office of Fusion Energy Science
Contract DE-SC0001939

Sandia National Laboratories

Thank you

References for rates and cross-sections

- **Superelastic**
  - Klein Rosseland
  - Sobelman

$$K_{ij}^{e} = \langle \sigma_{ij} v_e \rangle = \left(\frac{m_e}{2\pi k T_e} \right)^{3/2} \int_0^{\infty} \sigma_{ij}(v) \exp\left(\frac{-m_e v^2}{2 k_B T_e} \right) 4\pi v^2 dv \left[\frac{g_j}{g_i} \exp\left(\frac{(E_j - E_i)}{k_B T_e} \right) \right]$$

[1] C. F. Burrell and H.-J. Kunze, Phys. Rev. A **18**, 2081 (1978).
[1] P. Chall, E. K. Souw and J. Uhlenbusch. J. Quant. Spectrosc. Radiant. Transfer **34**, 309 (1985).
[1] G. Dilecce, P. F. Ambrico and S. De Benedictis, J. Phys. B: At. Mol. Opt. Phys. **28**, 209 (1994).
[1] R. Denkelmann, S.Maurmann, T. Lokajczyk, P. Drepper, and H. –J. Kunze, J. Phys. B: At. Mol. Opt. Phys. **32**, 4635 (1999).
[1] R. Denkelmann, S. Freund and S. Maurmann, Contrib. Plasma Phys. **40**, 91 (2000).
[1] K. Tsuchida, S. Miyake, K. Kadota and J. Fujita, Plasma Physics **25**, 991 (1983).
[1] B. Dubreuil and P. Prigent, J. Phys. B: At. Mol. Opt. Phys. **18**, 4597 (1985).
[1] E. A. Den Hartog, T. R. O'Brian and J. E. Lawler, Phys. Rev. Lett. **62**, 1500 (1989).
[1] K. Dzierzega, K. Musiol, E. C. Benck and J. R. Roberts, J. Appl. Phys. **80**, 3196 (1996).
[1] L. Maleki, B. J. Blasenheim, and G. R. Janik, J. Appl. Phys. **68**, 2661 (1990).
[1] R. S. Stewart, D. J. Smith, I. S. Borthwick and A. M. Paterson, Phys. Rev. E **62**, 2678 (2000).
[1] R. S. Stewart, D. J. Smith, J. Phys. D: Appl. Phys. **35**, 1777 (2002).
[1] A. Hidalgo, F. L Tabares and D. Tafalla, Plasma Phys. Control. Fusion **48**, 527 (2006).
[1] D. A. Shcheglov, S. I. Vetrov, I. V. Moskalenko, A. A. Skovoroda and D. A. Shuvaev, Plasma Phys. Rep. **32**, 119 (2006).
[1] M. Krychowiak, Ph Mertens, R. Konig, B. Schweer, S. Brezinsek, O. Schmitz, M. Brix, U. Samm and T. Klinger, Plasma Phys. Control. Fusion **50**, 65015 (2008).
[1] K. Takiyama, H. Sakai, M. Yamasaki, and T. Oda, Jpn. J. Appl. Phys. **33**, 5038 (1994).
[1] M. Watanabe, K. Takiyama, H. Toyota Jpn. J. Appl. Phys. **38**. 4380 (1999).
[1] G. Nersisyan, T. Morrow, and W. G. Graham, Appl. Phys. Lett. **85**, 1487 (2004)
[1] W. L Wiese, M. W. Smith, and B. M. Glennon, *Atomic Transition Probabilities **4/V1*** (Nat. Stand. Ref. Data. Ser., Nat. Bur. Stand. Washington DC, 1966).
[1] Yu. Ralchenko, R. K. Janev, T. Kato, D. V. Fursa, I. Bray, F. J. De Heer, Atomic Data and Nuclear Data Tables **94**, 603 (2008).
[1] I.I. Sobelman, L. A. Vainshtein, and E. A. Yukov, *Excitation of Atoms and Broadening of Spectral Lines* (Springer, New York, 1981) p. 5.

$$K_{ij}^{e} = \langle \sigma_{ij} v_e \rangle = \left(\frac{m_e}{2\pi k T_e} \right)^{3/2} \int_0^{\infty} \sigma_{ij}(v) \exp\left(\frac{-m_e v^2}{2 k_B T_e} \right) 4\pi v^3 dv$$

Calibration

Key uphill transitions are not significantly impacted by radioactive coupling

- **Dominant population pathway is still through excited 3^3P state**
  - Final densities of 3^3P state will change, but this is normalized out in analysis

Averaged trends

Data Set A: $A_{Eff} = A_{Nom}$

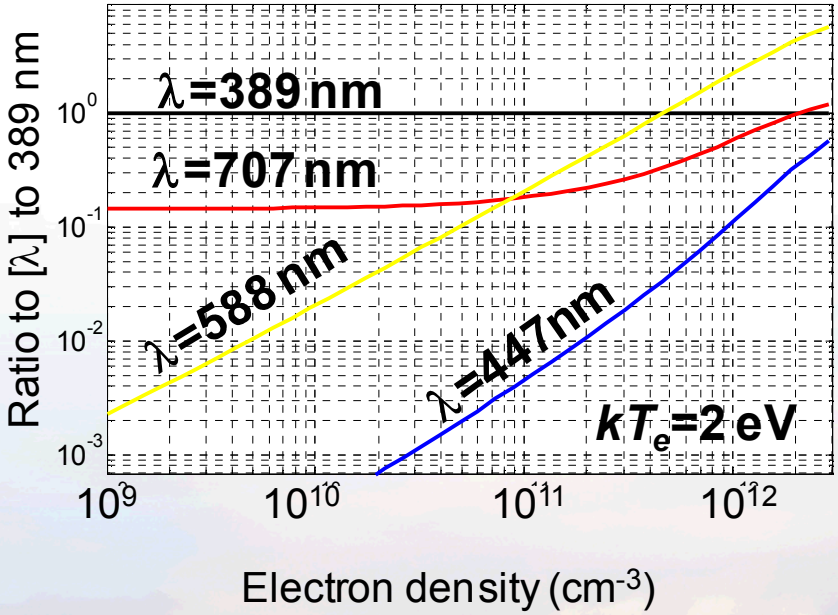

Data Set B: $A_{Eff} >> A_{Nom}$ (During laser excitation)

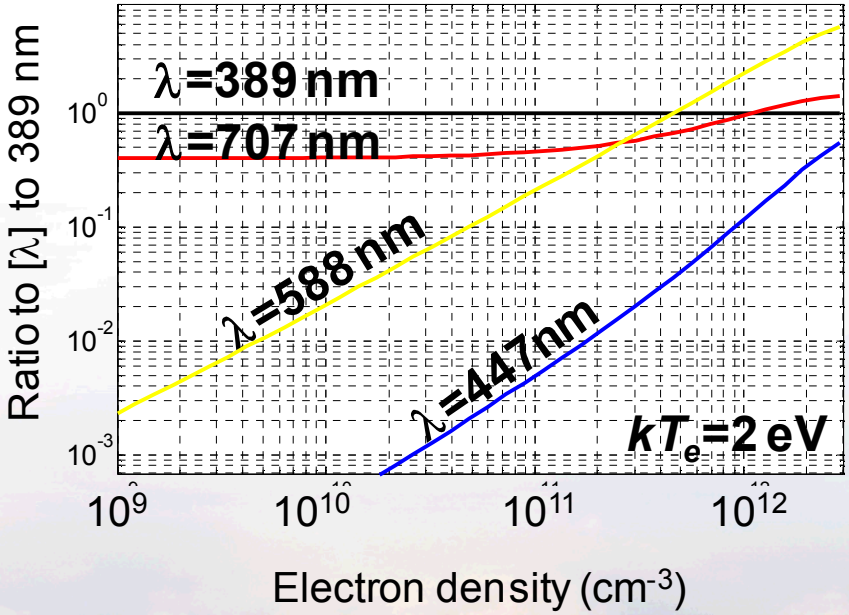

Caution should still be used if considering the 3^3S state for normalization

Sandia National Laboratories

[447]/[588] ratio captures trends but misses absolutes

- **Anticipated T_e trends are observed**
  - High temperature at start, low temperatures later on
- **Measure T_e trends mimic computed trends**
  - Discrepancy in absolute values are apparent

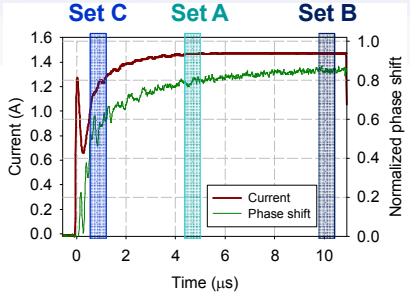

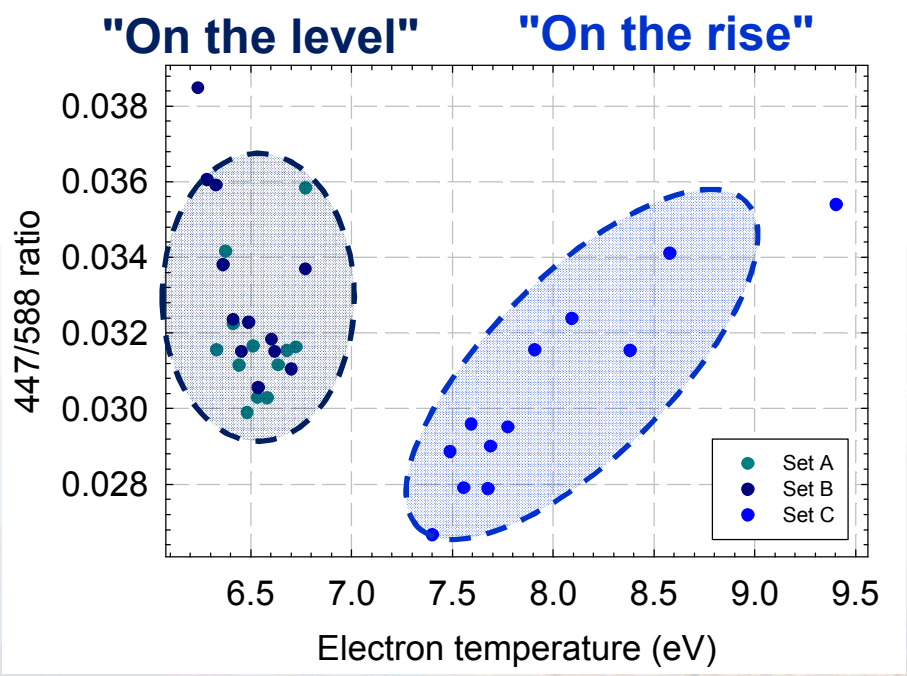

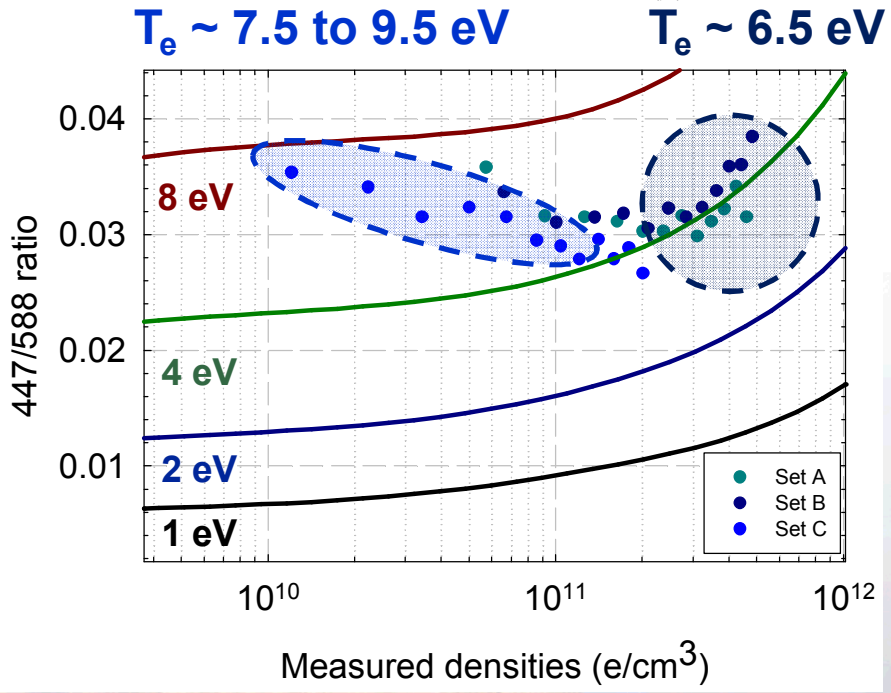

Uncertainties in rates, EEDF and/or interpolation of T_e from drift parameters should impact absolute values

Calibration of 2^3P excitation

Time dependent trends

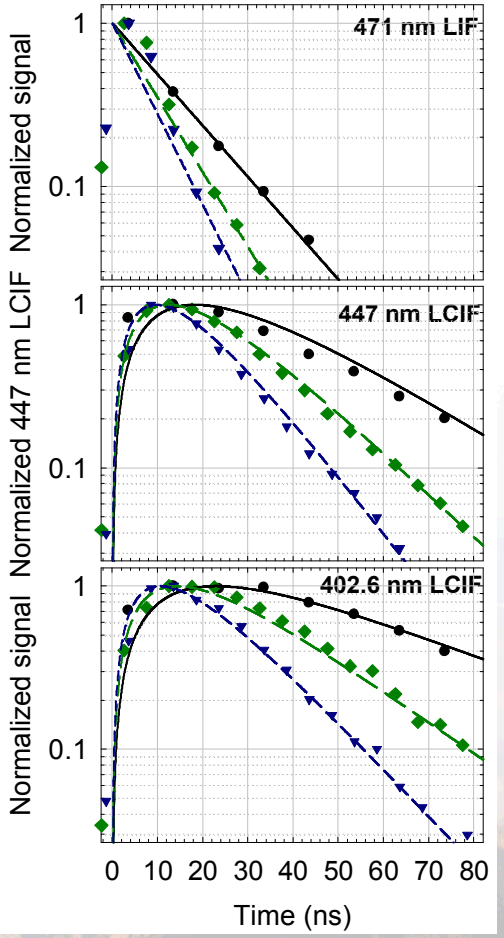

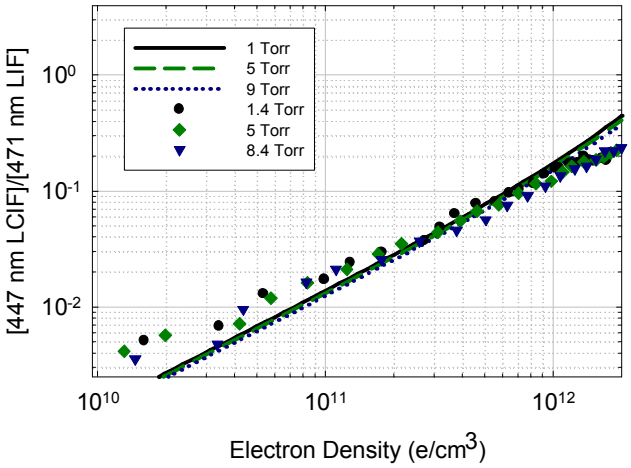

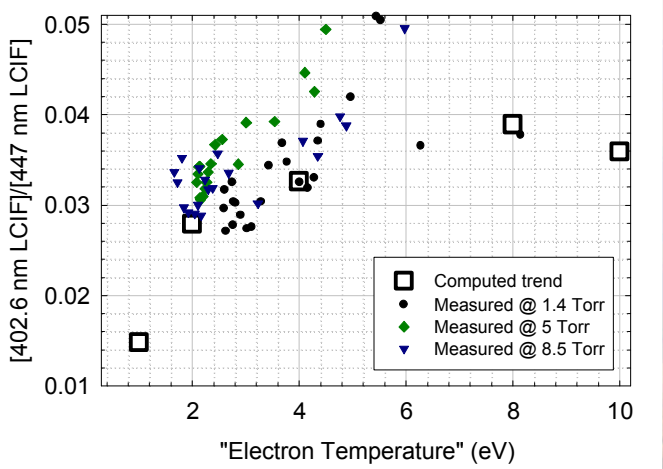

LCIF trends are consistent with computed rates

- **In afterglow electron temperature rapidly cools**
  - O(~1 μs)
- **Electron densities decay much slower**
  - O(~10's μs)
- **3^3D LCIF does not track 4^3D LCIF**
  - Does not demonstrate significant temperature dependence

Densities and temperatures

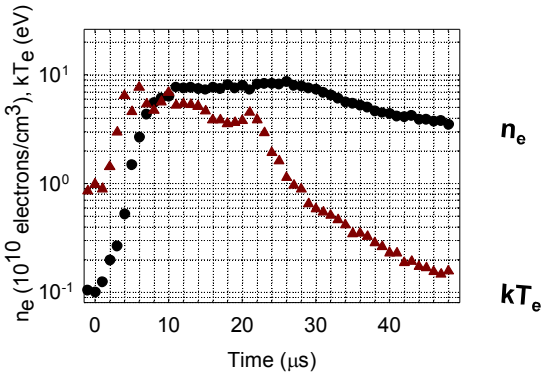

LCIF Trends

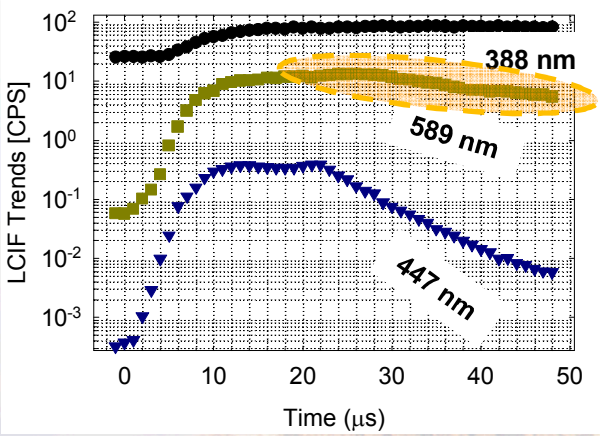

$3^3P \rightarrow 3^3S, 3^3D$

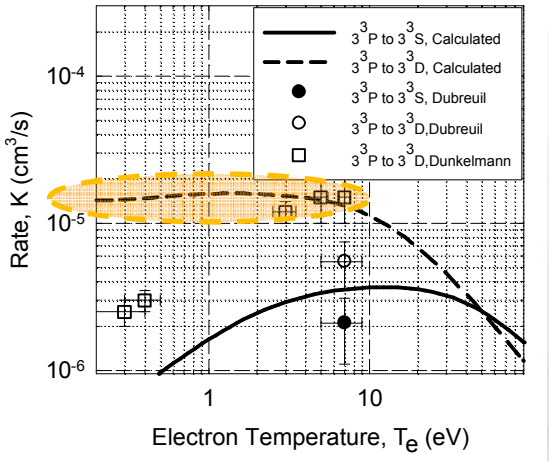

Densities and temperatures vary by orders of magnitude; rates demonstrate different time scales

Electrons backfill ion sheath after voltage is removed

- **LCIF detects electrons but not ions**
  - Examine time immediately after voltage is removed

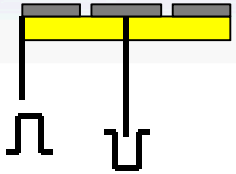

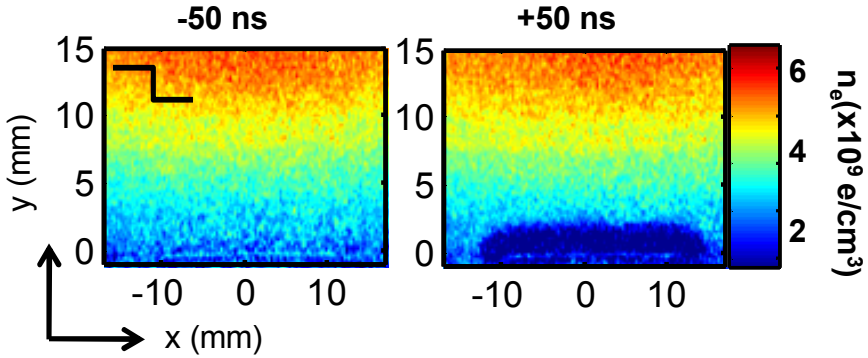

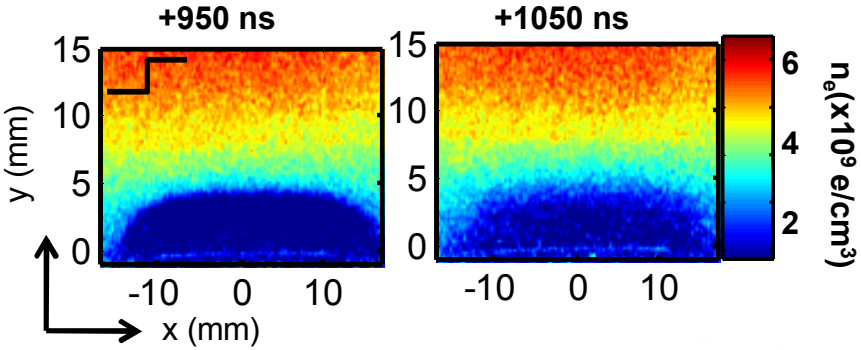

Negative Pulse

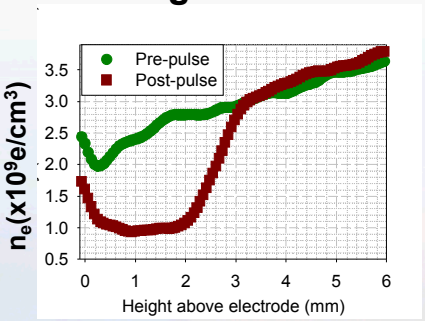

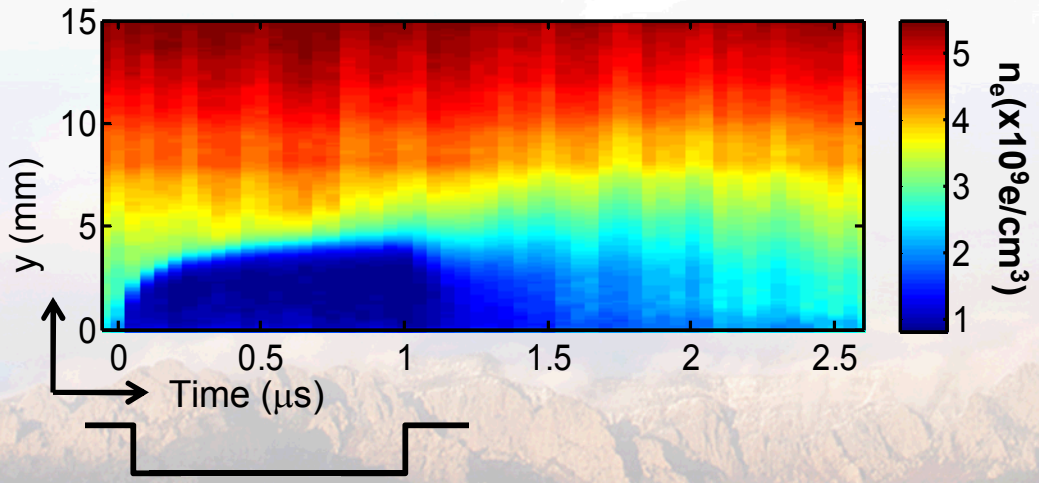

Positive Pulse

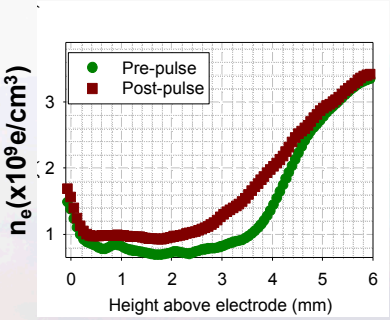

Ion densities can be quantified after voltage is removed

Sandia National Laboratories